



[Click here to view linked References](#)

1
2
3
4
5
6
7
8
9
10
11
12
13
14
15
16
17
18
19
20
21
22
23
24
25
26
27
28
29
30
31
32
33
34
35
36
37
38
39
40
41
42
43
44
45
46
47
48
49
50
51
52
53
54
55
56
57
58
59
60
61
62
63
64
65

1 **Biochemical inhibition of acid phosphatase activity in two mountain spruce forest soils**

2 **Petr Čapek^{*a}, Christopher P Kasanke^b, Robert Starke^c, Qian Zhao^b, Karolina Tahovská^a**

3

4 ^a*Department of Ecosystem Biology, Faculty of Science, University of South Bohemia,*

5 *České Budějovice, Czech Republic*

6 ^b*Environmental Molecular Sciences Laboratory, Pacific Northwest National Laboratory, Richland, WA USA*

7 ^c*Institute of Microbiology of the Czech Academy of Sciences, v. v. i., Vídeňská 1083, CZ 14220 Praha, Czech*

8 *Republic*

9

10 *Corresponding author: Petr Čapek: petacapek@gmail.com (ORCID ID 0000-0001-9362-6384)

11 Christopher P Kasanke: christopher.kasanke@pnnl.gov (ORCID ID 0000-0001-7940-0477)

12 Robert Starke: robert.starke@biomed.cas.cz (ORCID ID 0000-0003-3020-4605)

13 Qian Zhao: qian.zhao@pnnl.gov (ORCID ID 0000-0003-4489-3691)

14 Karolina Tahovská: tahovska@centrum.cz (ORCID ID 0000-0003-4499-9533)

1
2
3
4
5
6
7
8
9
10
11
12
13
14
15
16
17
18
19
20
21
22
23
24
25
26
27
28
29
30
31
32
33
34
35
36
37
38
39
40
41
42
43
44
45
46
47
48
49
50
51
52
53
54
55
56
57
58
59
60
61
62
63
64
65

15 **Abstract**

16 The product inhibition of the 4-Methylumbelliferyl phosphate (MUB-P) decay rate, a measure of potential acid
17 phosphatase activity, has not been considered in most of the published kinetic studies. The aim of this study was to
18 determine the type and strength of the product inhibition in order to better define reaction conditions at which the
19 acid phosphatase activity assay produces unbiased results. The MUB-P decay rate was measured in the forest floor
20 and topsoil organic horizons of two spruce forest catchments at different initial MUB-P and $P-PO_4^{3-}$ concentrations.
21 The type and strength of the inhibition was analyzed by non-linear regression. We found that MUB-P decay was
22 competitively inhibited by the $P-PO_4^{3-}$ but also by dissolved organic P. By using estimated kinetic parameters, we
23 calculated an underestimation of potential acid phosphatase activity by up to ~20% at concentrations of added
24 MUB-P as high as $300 \mu\text{mol g}^{-1}$ dry weight and an incubation time one hour due to background inorganic and
25 organic P concentrations in range of units of μmol per gram of dry soil. We discuss approaches that can be used to
26 minimize the underestimation and show that the previously defined recommendations might not be always sufficient
27 to avoid the bias. Therefore, we recommend to analyze progress curves at a wide range of initial MUB-P
28 concentrations using non-linear methods when the enzyme assay is optimized for a given soil. When changes in
29 inorganic and/or organic P concentrations are expected, we further recommend measuring background inorganic and
30 organic P concentrations.

1
2
3
4 31 **Key words**

5
6 32 Enzyme assay, soil acid phosphatases, biochemical inhibition, linear regression, Michaelis-Menten kinetic
7
8

9 33 **Introduction**

10 34 The decay rate of artificial substrates are frequently reported in soil studies as an estimate of the potential activity of
11
12 35 an enzyme class of interest (e.g. acid phosphatases, acetyl esterase, leucin aminopeptidase, etc.; Allison and
13
14 36 Vitousek 2005; German et al. 2011; Olander and Vitousek 2000). This decay rate is measured as an increase of
15
16 37 reaction product concentration over time and it is assumed to follow Michaelis-Menten kinetics (e.g. German et al.
17
18 38 2011; Malcolm 1983; Margenot et al. 2018) described in eq. 1:

19
20
21 39
$$\frac{dProduct}{dt} = \frac{V_{MAX} \times S}{K_M + S}, \quad (1)$$

22
23

24 40 in which, V_{MAX} is the apparent maximum velocity constant, S is substrate concentration, K_M is the apparent affinity
25
26 41 constant, $Product$ is concentration of a reaction product and t is time (Figure 1A). When performing an enzyme
27
28 42 assay, it is common practice to add a saturating amount of a substrate to the soil-buffer slurry. At the saturating
29
30 43 substrate concentration, the slope of the increase in reaction product concentration over time ($dProduct/dt$) can be
31
32 44 estimated using a linear regression or linear two-point interpolation and becomes equal to V_{MAX} because the reaction
33
34 45 follows zero-order kinetic (Figure 1B, C; e.g. German et al. 2011). This rate is denoted as a potential enzyme
35
36 46 activity.

37
38
39 47 At present, large ambiguity surrounds the way the measured potential enzyme activity should be interpreted
40
41 48 (German et al. 2011; Nannipieri et al. 2018). Whereas some studies assume that the potential enzyme activity
42
43 49 reflects activity of enzymes located outside of the cell and as such, can be used to determine nutrient limitation and
44
45 50 carbon use efficiency of soil microbial communities (Malik et al. 2019; Sinsabaugh et al. 2013), other studies
46
47 51 advocate for more careful interpretations (Nannipieri et al. 2018; Rosinger et al. 2019). As argued by Nannipieri et
48
49 52 al. (2018), it cannot be assumed that the enzymes located outside the cell are solely responsible for the decay of an
50
51 53 artificial substrate. Thus, the measured enzyme activity rather represents the potential of a soil to perform a specific
52
53 54 reaction, which is, however, never reached *in-situ*. Even though the assay conditions such as temperature and pH can
54
55 55 be manipulated to represent field conditions, it is unclear whether the artificial substrate decay has the same reaction
56
57 56 kinetic as the organic compounds present in soil.
58
59
60
61
62
63
64
65

1
2
3
4 57 In the past, several methodological studies have been published to provide recommendations for the
5
6 58 enzyme activity assay optimization (e.g. German et al. 2011; Malcolm 1983; Margenot et al. 2018; Verchot and
7
8 59 Borelli 2005). Particular attention was paid to defining concentration of an artificial substrate added to a soil-buffer
9
10 60 slurry at which the reaction follows zero order kinetic so the linear regression without the intercept can be used to
11
12 61 determine unbiased V_{MAX} . Specifically, estimation with zero order kinetic requires S being much higher than $K_M +$
13
14 62 S . When S is much lower than K_M , the reaction follows first order kinetic. By definition, linear regression can then
15
16 63 be used only to estimate $\frac{V_{MAX}}{K_M}$ as a slope of increase of natural logarithm of the product concentration over time. It
17
18
19 64 was recommended to add concentration at least five times greater than the value of K_M (Malcolm 1983; Margenot et
20
21 65 al. 2018). Within the initial linear region of product concentration increase over time, the estimated potential enzyme
22
23 66 activity is equal to 83% of V_{MAX} at such conditions according to eq. 1.

25 67 Eq. 1, however, is absent of any inhibition term. Biochemical inhibition by the reaction product is
26
27 68 frequently reported for isoenzymes belonging to all major classes of hydrolytic enzymes commonly measured in soil
28
29 69 including cellobiosidases, β -glucosidases (Gusakov and Sinitsyn 1992), β -N-acetylglucosidases (Vötsch and
30
31 70 Templin 2000), aminopeptidases (Gilboa et al. 2001), and especially phosphatases (Bezerra and Dias 2007; Gerritse
32
33 71 and van Dijk 1978; Kiffer-Moreira et al. 2007; Pang and Kolenko 1986; Spiers and McGill 1979;). When the
34
35 72 reaction is inhibited by the product, its rate slows down over time as the product concentration increases (see Figure
36
37 73 1B and Supplementary Information, section 1). Increasing product concentration causes an increase of the K_M value
38
39 74 (Figure 1A) thus, pushing the reaction away from zero order kinetic. As a result, a linear regression may
40
41 75 underestimate the potential enzyme activity depending on the duration of the reaction, strength and type of the
42
43 76 inhibition, substrate concentration, and initial concentration of an inhibitor (Figures 1 and SI-4). Since most
44
45 77 published kinetic studies conducted with soil samples implicitly neglected biochemical inhibition providing only the
46
47 78 “apparent” kinetic constants of eq. 1 (e.g. Arevalo et al. 1993; Batistic et al. 1980; Eivazi and Tabatabai 1977; Hui et
48
49 79 al. 2013; Juma and Tabatabai 1988; Khadem and Raiesi 2019; Leite et al. 2018; Malcolm 1983; Marx et al. 2001;
50
51 80 Nannipieri et al. 1982; Razavi et al. 2016; Stock et al. 2019; Stone and Plante 2014; Tan et al. 2020; Trasar-Cepeda
52
53 81 et al. 2007; Vuorinen and Saharinen 1996; Vuorinen 1999; Zhang et al. 2018), the strength of the biochemical
54
55 82 inhibition and thus, its implications for the enzyme assay are poorly defined.

57 83 The aim of this study was to quantify the effect of biochemical inhibition on 4-Methylumbelliferyl
58
59 84 phosphate (MUB-P) substrate decay, which is used to determine the acid phosphomonoesterase activity in acidic
60
61
62
63
64
65

1
2
3
4 85 soils. We specifically focused on acid phosphomonoesterases (hereafter denoted as acid phosphatases) since the
5
6 86 biochemical inhibition by the product ($P-PO_4^{3-}$) is likely to occur (Bezerra and Dias 2007; Gerritse and van Dijk
7
8 87 1978; Kiffer-Moreira et al. 2007; Pang and Kolenko 1986; Spiers and McGill 1979;). In this study, we used forest
9
10 88 floor and topsoil organic horizons of two adjacent mountain catchments, Plešné and Čertovo (Šumava Mts., Czech
11
12 89 Republic). Previous studies showed that regardless of similar vegetation, climatic conditions (Turek et al. 2014),
13
14 90 atmospheric P inputs (Kopáček et al. 2011) and litterfall C to P ratio (Kopáček et al. 2015), both catchments have
15
16 91 distinctly different *in-situ* P dynamic (Tahovská et al. 2018). It has been suggested that this difference could partly
17
18 92 result from different chemical composition of the bedrock (P rich granite at the Plešné catchment vs. P poor mica
19
20 93 schist at Čertovo catchment), but also from the different soil acid phosphatase activities (Šantrůčková et al. 2004;
21
22 94 Tahovská et al. 2018). The soils from these catchments thus, can differ in the presence and/or strength of
23
24 95 biochemical inhibition on acid phosphatase activity. We hypothesized, that the MUB-P decay rate is competitively
25
26 96 inhibited by the product. High background concentration of the product and its accumulation over time are
27
28 97 responsible for underestimation of the potential acid phosphatase activity estimated by a linear regression.
29
30

31 98 **Material and methods**

32 33 99 *Soils and forest floor samples*

34
35 100 Soils and forest floor were sampled in October 2019 in the catchments of the glacial lakes Plešné (48°77'N,
36
37 101 13°86'E) and Čertovo (49°16', 13°20'E) located in the Šumava Mountains in the south-western part of the Czech
38
39 102 Republic. The sampling was a part of regular six-week monitoring described in Kaňa et al. (2015) and thus, the
40
41 103 same sampling protocol was followed. Six randomly selected pits of the size 15×15 cm were excavated to a depth of
42
43 104 approx. 20 cm. Samples of diagnostic soil horizons denoted hereafter as a forest floor (Ol+Of, i.e. top ~5 cm
44
45 105 containing fragmented but visible plant litter remnants) and topsoil organic (H, i.e. between ~5 to 15 cm depth
46
47 106 containing amorphous organic material) horizons were collected. All samples were immediately sieved through 5
48
49 107 mm mesh. 5 mm mesh size was selected instead of 2 mm to pass plant litter fragments of forest floor through the
50
51 108 sieve as typically done in spruce forest ecosystems (e.g. Högberg et al. 2020; Giesler et al. 2002). Samples from two
52
53 109 randomly selected pits were mixed to create one composite sample. Thus, three composite samples of each horizon
54
55 110 were created from six excavated pits (Kaňa et al. 2015). All samples were kept at 4°C in the dark until the analyses
56
57 111 (approx. six months). The basic characteristics of the samples used in this study – i.e. pH, total organic C (C_T), total
58
59 112 N (N_T), K_2SO_4 extractable organic C (DOC), N (DON), exchangeable NH_4^+ and NO_3^- , microbial biomass C (MBC),
60
61
62
63
64
65

1
2
3
4 113 N (MBN) and P (MBP); were measured before the enzyme assay. Soil pH was measured in 1:2.5 (w/w) soil-water
5
6 114 slurry using portable pH meter 330i (Xylem Analytics, Weilheim, Germany). C_T and N_T were measured in dried (at
7
8 115 60°C to a constant weight) and finely ground (using a Mixer Mill MM 200, Retsch, Germany) samples using NC
9
10 116 2100 soil analyzer (Thermo Quest Italia S.p.A., Rodano, MI). To analyze DOC, DON, NO_3^- and NH_4^+ , five grams of
11
12 117 fresh soil samples were shaken with 20 mL of 0.5 M K_2SO_4 for one hour at laboratory temperature in the dark.
13
14 118 Extracts were centrifuged (3000 g) and filtered through 0.45 μ m glass fiber filters (Watrex, Prague, Czech Republic).
15
16 119 Total dissolved N and DOC in extracts were measured with a TOC/TN analyzer (LiquiTOC II, Elementar,
17
18 120 Germany). NO_3^- and NH_4^+ concentrations were measured spectrophotometrically using a flow injection analyzer
19
20 121 (QuickChem 8500, Lachat Instruments, USA). DON was calculated as the difference between total dissolved N and
21
22 122 the sum of NO_3^- and NH_4^+ concentrations (Tahovská et al. 2013).

23
24 123 MBC, MBN and MBP were analyzed by a fumigation-extraction method (Brookes et al. 1982, 1985; Vance
25
26 124 et al. 1987). The MBC and MBN were calculated as the difference in concentrations of their respective 0.5 M K_2SO_4
27
28 125 extractable forms in chloroform-treated (24 h) and untreated soil samples. Analogically, MBP was calculated as the
29
30 126 difference in $NaHCO_3$ extractable reactive P concentrations in chloroform-treated and untreated soil samples.
31
32 127 Calculated differences were corrected for incomplete extraction using the conversion factors 0.38, 0.54 and 0.4 for
33
34 128 MBC, MBN and MBP, respectively (Brookes et al. 1982, 1985; Vance et al. 1987). In addition, MBP was corrected
35
36 129 for the sorption of P released by chloroform treatment during extraction as described previously (Brookes et al.
37
38 130 1982).

41 131 *Acid phosphatase activity assay*

42
43 132 The assay was conducted according to general recommendations provided by German et al. (2011) and using 4-
44
45 133 Methylumbelliferyl phosphate (MUB-P) as a substrate, whose decay product (MUB) is fluorescent. This substrate
46
47 134 was selected mainly because the rapid and nearly continuous product formation can be measured (see below). The
48
49 135 disadvantage of this substrate, however, is the reduced sensitivity due to fluorescence intensity decrease at acidic pH
50
51 136 (Chrost and Krambeck, 1986). To prevent the bias associated with reduced sensitivity, the fluorescence –
52
53 137 concentration relationship was carefully calibrated for each soil sample (see below). The soil dilution and
54
55 138 homogenization was performed according to protocol used by Šantrůčková et al. (2004) for these soils. 100 mL of
56
57 139 buffer solution was added to one gram of the soil (~0.3 g oven-dry weight) and homogenized using an IKA Ultra-
58
59 140 Turrax T10 homogenizer (IKA®-Werke GmbH & Co. KG, Germany). All samples were treated similarly except
60
61
62
63
64
65

1
2
3
4 141 that the buffer pH was adjusted to pH of corresponding samples reported in Table 1. Because the soil pH range 3.5 –
5
6 142 4.5 measured across the samples (Table 1), 0.05 mol L⁻¹ citrate buffer, which is one of the main components of
7
8 143 universal buffer commonly used in previous studies (e.g. Drouillon and Merckx 2005; Juma and Tabatabai 1988;
9
10 144 Margenot et al. 2018; Spiers and McGill 1979; Trasar-Cepeda and Gil-Sotres 1988; Vuorinen and Saharinen 1996),
11
12 145 was selected. The stability of soil slurry pH over time was verified (data not shown).

14 146 While being stirred continuously, 200 µL of the soil slurry was pipetted into a 96-well plate followed by 50
15
16 147 µL of the solution containing MUB-P and KH₂PO₄ at different concentrations. 25 different solutions were prepared.
17
18 148 Five concentrations of MUB-P (3, 6, 16, 31, and 63 µmol MUB-P g⁻¹ dry weight) were combined with five
19
20 149 concentrations of P-PO₄³⁻ (0, 1, 6, 8, and 16 µmol P-PO₄³⁻ g⁻¹ dry weight). Every combination of MUB-P and P-
21
22 150 PO₄³⁻ was replicated three times. To control for spontaneous MUB-P decay, the same five concentrations of MUB-P
23
24 151 without P-PO₄³⁻ were added to 200 µL of the buffer solution. 200 µL of soil-buffer slurry from each soil sample was
25
26 152 further supplemented with 50 µL of the MUB standards at five different concentrations (5, 25, 50, 125, and 250
27
28 153 µmol MUB L⁻¹) or the buffer solution (i.e. representing the blank). The fluorescence of MUB standards was used to
29
30 154 account for product quenching and to calculate concentration of MUB produced by the enzymatic transformation of
31
32 155 MUB-P substrate.

34 156 The fluorescence intensity (i.e. excitation at 360 nm and emission at 460 nm wavelength, Drouillon and
35
36 157 Merckx 2005) of MUB was measured using a Spark microplate reader (Tecan Group Ltd., Männedorf, Switzerland).
37
38 158 To allow accurate determination of acid phosphatase kinetic parameters, the fluorescence was read at fine temporal
39
40 159 scale multiple times after the initiation of the reaction for up to 120 minutes (e.g. Perdicakis et al. 2004). This was
41
42 160 accomplished by measuring the background fluorescence in all wells without the presence of MUB-P/P-PO₄³⁻
43
44 161 solutions and then adding the solutions one-by-one, starting with the lowest concentration, and measuring
45
46 162 immediately. The time between the respective MUB-P/P-PO₄³⁻ addition and the first fluorescence reading was
47
48 163 approximately 40 seconds. The fluorescence was measured every minute for first 10 minutes and then after 15, 30,
49
50 164 45, 60, 75, 90, and 120 minutes. Between measurements, the plate was covered to prevent water loss and kept in the
51
52 165 dark at laboratory temperature (24°C). MUB concentration was calculated using a soil specific calibration and
53
54 166 corrected for spontaneous decay measured in the buffer solution (German et al. 2011).

56
57
58 167 *Determining the inorganic and organic P in citrate buffer*

1
2
3
4 168 Concentration of inorganic and organic P was measured in citrate buffer to determine initial reaction conditions of
5
6 169 acid phosphatase activity assay. The citrate buffer was prepared with five concentrations of P-PO₄³⁻ corresponding to
7
8 170 the concentration of P-PO₄³⁻ added to soil-buffer slurry with MUB-P. The same protocol described above was
9
10 171 followed. 100 mL of citrate buffer solutions were added to one gram of the soil and homogenized. After
11
12 172 homogenization, the soil-buffer slurry was filtered through 0.45µm glass fiber filters (Watrex, Prague, Czech
13
14 173 Republic) and the concentration of inorganic and organic P was measured. Soluble reactive P representing the
15
16 174 inorganic P was measured spectrophotometrically (Murphy and Riley 1962) using GENESYS™ 10S UV-Vis
17
18 175 Spectrophotometer (Thermo Fisher Scientific, Waltham, Massachusetts, USA). Total dissolved P was determined
19
20 176 for three concentrations of added P-PO₄³⁻ (0, 8, and 16 µmol P-PO₄³⁻ g⁻¹ dry weight) by perchloric acid digestion and
21
22 177 the molybdate method (Kopáček and Hejzlar 1993). Dissolved organic P was calculated as the difference between
23
24 178 total dissolved and soluble reactive P (Čapek et al. 2021).

27 179 *Data analysis and statistical evaluation*

29 180 *Linear regression*

31 181 Enzyme activity is typically estimated using a linear regression without the intercept. It must be ensured, however,
32
33 182 that the progress curve is within the linear region (German et al. 2011). Due to the design of acid phosphatase
34
35 183 activity assay, we calculated the enzyme activity using the linear regression within the shortest time interval we
36
37 184 could define (i.e. within the first five minutes). These values represent the instantaneous MUB-P decay rate specific
38
39 185 to respective reaction conditions (e.g. Reytor González et al. 2017). The effect of the P-PO₄³⁻ on acid phosphatase
40
41 186 activity was calculated for each combination of MUB-P and P-PO₄³⁻ concentration as the percentage in respect to
42
43 187 enzyme activity when no P-PO₄³⁻ was added to a respective MUB-P.

45 188 The fit of the linear regression was further studied in detail in samples supplemented by the highest (i.e.
46
47 189 saturating) concentration of MUB-P substrate and no added P-PO₄³⁻ which corresponds to the standard acid
48
49 190 phosphatase activity assay procedure (German et al. 2011). The saturating character of the highest MUB-P
50
51 191 concentration was verified beforehand (Figure SI-5). First, the linear regression was conducted over the whole
52
53 192 reaction time interval (i.e. from initiation of the reaction until the end). Within this interval, the presence of
54
55 193 significant breakpoint, at which the slope of product increase over time changes, was analyzed using the piecewise
56
57 194 linear regression (segmented R package version 0.5-4.0; Muggeo 2003). When this breakpoint was found, the acid
58
59 195 phosphatase activity was calculated for two time intervals separated by the breakpoint.

1
2
3
4 196 *Determining the product inhibition*

5
6 197 To analyze the presence of product (P-PO₄³⁻) inhibition, an integrated form of eq. 1 (denoted as WI – without
7
8 198 inhibition) was fitted to the progress curve data across all 25 combinations of initial substrate (MUB-P) and
9
10 199 inorganic P, separately for each soil. The goodness of fit was compared to the fit of integrated forms of equation 2
11
12 200 representing three different forms of product inhibition (Bezerra and Dias 2007):
13
14

15 201
$$\frac{dProduct}{dt} = \frac{V_{MAX} \times MUB-P}{K_M \times (1 + Product/K_{ic}) + MUB-P \times (1 + Product/K_{iu})} \quad (2)$$

16
17
18

19 202 In eq. 2, *K_{ic}* and *K_{iu}* are apparent inhibition constants, *MUB-P* is the substrate and *Product* is the reaction
20
21 203 product concentration (P-PO₄³⁻ produced in 1:1 to MUB). When both *K_{ic}* and *K_{iu}* are less than infinite, the product
22
23 204 inhibition is noncompetitive (denoted as NCI). Alternatively, *K_{iu}* or *K_{ic}* can be set infinite. When this is done, the
24
25 205 term in the respective parenthesis becomes one and the constant is eliminated from the eq. 2. When the *K_{iu}* constant
26
27 206 is eliminated, product inhibition becomes competitive (denoted as CI; Bezerra and Dias 2007). When *K_{ic}* is
28
29 207 eliminated, product inhibition becomes uncompetitive (denoted as UCI; Bezerra and Dias 2007).
30

31 208 The integrated forms of eqs. 1 and 2 listed in Table S1 didn't allow for the expression of the increase in
32
33 209 product concentration over time as a function of *V_{MAX}*, *K_M*, *K_{ic}*, and *K_{iu}* directly. Nevertheless, they allowed us to
34
35 210 match the measured concentration of the reaction product to a time point at which such a concentration should
36
37 211 theoretically appear based on respective initial concentration of MUB-P, inorganic P, *V_{MAX}*, *K_M*, *K_{ic}*, and *K_{iu}*. Thus,
38
39 212 the predicted variable was time and the explanatory variables were MUB-P and inorganic P concentrations at *t* = 0,
40
41 213 and product concentration at respective time *t*. The equation parameters *V_{MAX}*, *K_M*, *K_{ic}*, and *K_{iu}* were estimated using
42
43 214 non-linear least squares regression. To reduce the number of estimated parameters, *K_{iu}* was assumed to be equal to
44
45 215 *K_{ic}* for the NCI equation (Bezerra and Dias 2007). The goodness of fit of the integrated forms of eqs. 1 and 2 were
46
47 216 statistically compared using a standard Likelihood-ratio test. Each replicate was considered as a single measurement.
48
49

50 217 *Determining the inhibition by organic P*
51

52 218 MUB-P decay rate can be further inhibited by the soil organic P, if the acid phosphatases preferentially interact with
53
54 219 soil organic P rather than the MUB-P. Even though the initial organic P was not measured for all treatments, the
55
56 220 tight relationship between the added P-PO₄³⁻ and organic P concentrations depicted on figure 2B allowed us to
57
58 221 calculate initial organic P concentration for all treatments with high accuracy.
59
60
61
62
63
64
65

222 We tested two scenarios of MUB-P decay rate inhibition by organic P (denoted as DOP in eqs. 3 – 9). The
 223 first scenario is represented by differential equations (3) – (5):

$$224 \frac{dProduct}{dt} = \frac{V_{MAX} \times MUB-P}{K_{M-MUB-P} \times (1 + DOP/K_{M-DOP}) + MUB-P} \quad (3)$$

$$225 \frac{dMUB-P}{dt} = - \frac{V_{MAX} \times MUB-P}{K_{M-MUB-P} \times (1 + DOP/K_{M-DOP}) + MUB-P} \quad (4)$$

$$226 \frac{dDOP}{dt} = - \frac{V_{MAX} \times DOP}{K_{M-DOP} \times (1 + MUB-P/K_{M-MUB-P}) + DOP} \quad (5)$$

227 In these equations, $K_{M-MUB-P}$ and K_{M-DOP} represent apparent affinity constants specific to MUB-P and organic P,
 228 respectively. When $K_{M-MUB-P}$ is greater than K_{M-DOP} , acid phosphatases preferentially interact with organic P and
 229 decay rate of MUB-P substrate decreases similarly as in the case of competitive product inhibition. However, as the
 230 organic P concentration decreases over time (eq. 5), the MUB-P decay rate increases.

231 The second scenario is represented by differential equations (6) – (9) and extends the first scenario by
 232 accounting for competitive product inhibition described above:

$$233 \frac{dMUB}{dt} = \frac{V_{MAX} \times MUB-P}{K_{M-MUB-P} \times (1 + SRP/K_{ic}) \times (1 + DOP/K_{M-DOP}) + MUB-P} \quad (6)$$

$$234 \frac{dMUB-P}{dt} = - \frac{V_{MAX} \times MUB-P}{K_{M-MUB-P} \times (1 + SRP/K_{ic}) \times (1 + DOP/K_{M-DOP}) + MUB-P} \quad (7)$$

$$235 \frac{dDOP}{dt} = - \frac{V_{MAX} \times DOP}{K_{M-DOP} \times (1 + SRP/K_{ic}) \times (1 + MUB-P/K_{M-MUB-P}) + DOP} \quad (8)$$

$$236 \frac{dSRP}{dt} = \frac{V_{MAX} \times MUB-P}{K_{M-MUB-P} \times (1 + SRP/K_{ic}) \times (1 + DOP/K_{M-DOP}) + MUB-P} + \frac{V_{MAX} \times DOP}{K_{M-DOP} \times (1 + SRP/K_{ic}) \times (1 + MUB-P/K_{M-MUB-P}) + DOP} \quad (9)$$

237 Thus, the MUB-P decay rate (eqs. 6 and 7) is inhibited by the product and organic P. In this scenario, it was
 238 necessary to distinguish between two products of MUB-P decay – fluorescent MUB (eq. 6), which is directly
 239 measured, and $P-PO_4^{3-}$ (denoted as SRP – eq. 7 – 9), which is released from MUB-P in 1:1 to MUB. Whereas MUB
 240 is produced by the decay of MUB-P (eq. 6), $P-PO_4^{3-}$ is produced by both MUB-P and organic P decay (eq. 9).

1
2
3
4 241 Since differential eqs. 3 – 9 cannot be integrated analytically, a numerical solution method was used
5
6 242 (deSolve R package version 1.21; Soetaert et al. 2010). The models were parametrized against the product
7
8 243 concentration across all 25 combinations of initial MUB-P and P-PO₄³⁻ concentrations and the entire reaction time
9
10 244 using the Artificial Bee Colony algorithm (ABCoptim R package version 0.15.0; Vega Yon and Muñoz 2017)
11
12 245 minimizing the residual sum of squares normalized to initial MUB-P concentrations. The goodness of fit of both
13
14 246 models (eqs. 3 – 5 and eqs. 6 – 9) was compared with previously parametrized CI model using the Likelihood-ratio
15
16 247 test. All data analyses were done in the statistical program R version 3.6.3 (R Core Team 2020). All code and data
17
18 248 necessary to reproduce our results are available at https://github.com/petacapek/Enzyme_inhibition.

21 249 **Results**

23 250 *Soil and forest floor characteristics*

25 251 All samples were highly acidic (Table 1). The soil pH ranged from 3.58 to 4.51. The concentrations of inorganic and
26
27 252 organic P was generally higher in forest floor samples as compared to organic topsoils. Similarly, C_T, N_T, MBC,
28
29 253 MBN and MBP were higher in forest floor samples as compared to organic topsoils.

32 254 *Biochemical product inhibition determination*

34 255 The inorganic P concentration in the soil-buffer slurry was close to the amount of added P-PO₄³⁻ (Figure 2A). At the
35
36 256 highest additions of KH₂PO₄, the measured inorganic P concentration matched added amount of P-PO₄³⁻ almost
37
38 257 exactly. At lowest KH₂PO₄ additions, however, the measured inorganic P concentration always exceeded the amount
39
40 258 of added P-PO₄³⁻. The difference between the measured inorganic P and added P-PO₄³⁻ was accounted for in all
41
42 259 models. Organic P concentration in the soil-buffer slurries was not constant across increasing concentrations of
43
44 260 added P-PO₄³⁻. Organic P increased with increasing concentration of added P-PO₄³⁻ (Figure 2B) and was
45
46 261 approximately two to three times lower than inorganic P.

48 262 All three forms of integrated eq. 2 fitted the progress curve data significantly better than the integrated form
49
50 263 of eq. 1 regardless of soil sample (Table 2). In all soil samples, the regression analysis indicated that the competitive
51
52 264 product inhibition (CI) described the data with the highest accuracy. However, there was disagreement between the
53
54 265 actual and estimated effect of inorganic P on enzyme activity, especially in forest floor horizons (Figure 3). The
55
56 266 enzyme activity at the two lowest concentrations of MUB-P was lower than expected by the CI model.

59 267 *Linear regression analysis and organic P inhibition*

1
2
3
4 268 At the highest MUB-P concentration, piecewise linear regression indicated the presence of significant breakpoints in
5
6 269 the product concentration increase over time (Figure 4). In forest floor horizons, this breakpoint appeared within the
7
8 270 first ~20 minutes of the reaction time. In organic topsoil horizons, it appeared after one hour. The two time intervals
9
10 271 separated by the breakpoint had different slopes of product increase over time, but this difference was opposite of
11
12 272 what we expected. In the later time interval, the slope increased by ~20 and ~10% in forest floor and organic topsoil
13
14 273 horizons, respectively (Figure 4).

15
16 274 The models acknowledging inhibition of MUB-P decay by the preferential interaction of acid phosphatases
17
18 275 with organic P (described in eqs. 3 – 5 and 6 – 9) generally outperformed the CI model in terms of ability to
19
20 276 simulate the increase of product concentration over time and across all combinations of initial MUB-P and $P-PO_4^{3-}$
21
22 277 concentrations (Table 3). In the forest floor horizon of Plešné catchment, only the preferential interaction of acid
23
24 278 phosphatases with organic P (eqs. 3 – 5) was able to explain most of the variability in the data. The apparent affinity
25
26 279 constant for organic P (K_{M-DOP}) was ~3 times lower than the apparent affinity constant for MUB-P ($K_{M-MUB-P}$, Table
27
28 280 3). In the other three soil samples, a combination of preferential interaction of acid phosphatases with organic P and
29
30 281 biochemical competitive product inhibition (eqs. 6 – 9) had to be acknowledged to better simulate product
31
32 282 concentration increase over time (Table 3). In both horizons from the Čertovo catchment, the dominant effect on
33
34 283 MUB-P decay was exhibited by organic P as indicated by lower K_{M-DOP} compared to $K_{M-MUB-P}$. The inorganic P
35
36 284 concentration effect on MUB-P decay rates was more prevalent in the organic topsoil horizon from the Plešné
37
38 285 catchment.

40 41 286 **Discussion.**

42 43 287 *Biochemical product inhibition*

44
45 288 The experimental setup of this study was specifically designed to determine the biochemical inhibition of acid
46
47 289 phosphatase activity by the reaction product (i.e. $P-PO_4^{3-}$). According to our hypothesis, the decay rate of MUB-P
48
49 290 substrate, which is specific to the acid phosphatase enzyme class, decreased with increasing $P-PO_4^{3-}$ (Figure 3). The
50
51 291 regression analysis suggested the presence of competitive product inhibition (Table 2). This finding is consistent
52
53 292 with other studies implying that competitive inhibition by the reaction product is prevalent for acid phosphatases
54
55 293 (Bezerra and Dias 2007; Gerritse and van Dijk 1978; Kiffer-Moreira et al. 2007; Pang and Kolenko 1986; Spiers and
56
57 294 McGill 1979;). As suggested by crystallographic studies, competitive product inhibition seems to be inherent to all
58
59 295 phosphatases due to the architecture of their active sites (Anand and Srivastava 2012; Mitić et al. 2006; Sunden et al.

1
2
3
4 296 2016). Phosphatases are binuclear metallohydrolases therefore, their active sites consist of two metal atoms (Fe, Mn
5
6 297 or Zn) which bind organic P by its the terminal phosphate group (Anand and Srivastava 2012; Mitić et al. 2006).
7
8 298 Once the ester bond between the phosphate and organic residue is broken due to the nucleophilic attack, phosphate
9
10 299 remains in the active site and must be displaced to allow enzyme regeneration (e.g. Mitić et al. 2006; Sunden et al.
11
12 300 2016). Phosphate displacement is considered a rate limiting step of the reaction (Mitić et al. 2006). When the
13
14 301 targeted mutations impair the ability of active site to displace phosphate, the reaction rate decreases whereas strength
15
16 302 of competitive product inhibition increases (Sunden et al. 2016).

17
18 303 Because the enzyme assay was conducted within two hours, it is unlikely that the decrease of MUB-P
19
20 304 decay rate along the gradient of increasing $P-PO_4^{3-}$ concentration was caused by repression of the acid phosphatases
21
22 305 production, which has been observed in previous studies (Nannipieri et al. 1978; Spiers and McGill 1979; Yoshida
23
24 306 et al. 1989). The decay and/or production of acid phosphatases should affect the MUB-P decay rate at longer time
25
26 307 scales (Nannipieri et al. 2011; Schimel et al. 2017; Spiers and McGill 1979).

27
28 308 Further, we found indications suggesting that the inorganic P concentration might not be the only factor
29
30 309 responsible for decrease in MUB-P decay rate. First, the MUB-P decay rate decreased with increasing initial
31
32 310 inorganic P concentration more than expected by the competitive inhibition model exclusively (Figure 3). Second,
33
34 311 the MUB-P decay rate increased over time at the highest MUB-P concentration (Figure 4). If product inhibition is
35
36 312 the only mechanism affecting the MUB-P decay rate, a decrease in the MUB-P decay rate over time should be
37
38 313 observed instead. The accelerated MUB-P decay rate cannot be simply explained by decreasing inorganic P
39
40 314 concentration over time via sorption to soil particles because the inorganic P concentration tended to increase over
41
42 315 time at all initial $P-PO_4^{3-}$ concentrations (Figure SI-6) and moreover, citrate buffer should prevent re-adsorption of
43
44 316 inorganic P to mineral soil particles in acidic soils. Also, the increase in slope of the linear regression was higher for
45
46 317 forest floor horizons at which the adsorption should be lower. All lines of evidences suggest that the MUB-P decay
47
48 318 was also inhibited due to preferential interaction of acid phosphatases with organic P.

51 52 319 *Inhibition by preferential interaction of acid phosphatases with organic P*

53
54 320 The initial concentrations of organic and inorganic P were correlated (Figure 2). Thus, the effects of both P forms on
55
56 321 the MUB-P decay rate should multiply with increasing concentration of $P-PO_4^{3-}$ added to soil-buffer slurry. Indeed,
57
58 322 such a multiplicative effect was observed (Figure 3). In the forest floor horizon of the Čertovo catchment for
59
60 323 example, the MUB-P decay rate decreased to almost zero at the lowest MUB-P concentration (Figure 3). The

1
2
3
4 324 inhibition of MUB-P decay by organic P could further explain the acceleration of MUB-P decay rate over time. The
5
6 325 inhibition by organic P was greatest at the beginning of the reaction when the organic P concentration was the
7
8 326 highest. As the organic P was preferentially degraded by acid phosphatases, its concentration decreased over time.
9
10 327 Thus, the inhibiting effect decreased and ultimately increased the MUB-P decay rate.

11
12 328 Acid phosphatases are non-specific, they are able to catalyze hydrolysis of wide variety of phosphorylated
13
14 329 esters (Anand and Srivastava 2012). It is thus reasonable to expect a competition between organic P and MUB-P for
15
16 330 the enzyme active site by a same mechanism described for inorganic P. We therefore defined two models (eqs. 3 – 5
17
18 331 and 6 – 9) that acknowledged the competition between MUB-P and organic P for acid phosphatases to further
19
20 332 support all lines of evidences described above. Both models simulated the increase of product concentration over
21
22 333 time across all treatments with the similar or higher accuracy than competitive inhibition model (Table 2). In three
23
24 334 out of four soils, the estimated models' parameters suggested the higher affinity of acid phosphatases to organic P
25
26 335 compared to MUB-P (Table 2). This is not surprising given that the acid phosphatases should be designed to acquire
27
28 336 P from soil organic matter, not the artificial MUB-P substrate.

29
30 337 We also tested several alternative hypotheses that could theoretically explain the observed disagreements
31
32 338 between the expected effects of inorganic P on MUB-P decay and actual measurement (Fig. 3). These included (i)
33
34 339 combination of competitive product inhibition and substrate inhibition (Steen and Ziervogel 2012), (ii) cooperativity
35
36 340 mechanism in respect to substrate and product (Kellershohn and Laurent 1985), (iii) non-constant concentration of
37
38 341 acid phosphatases in time or (iv) two pools of acid phosphatases with different kinetic parameters acting on MUB-P
39
40 342 substrate (Nannipieri et al. 1982). However, none of these hypotheses was able to outperform the competitive
41
42 343 inhibition model (data not shown) leading us to a conclusion that the most parsimonious explanation of observed
43
44 344 patterns of MUB-P decay across our experimental treatments was the combination of competitive product inhibition
45
46 345 and preferential interaction of soil acid phosphatases with organic P.

47
48 346 There could be several reasons why our kinetic analysis failed to identify more than a single pool of acid
49
50 347 phosphatases acting on the MUB-P substrate even though presence of at least two pools can be expected (Nannipieri
51
52 348 et al. 1982). Different pools could have been present but they had similar apparent affinity and inhibition constants
53
54 349 in respect to inorganic and organic P. In such a case, the estimated V_{MAX} was a combination of different maximum
55
56 350 velocity constants of different enzyme pools. Alternatively, the single pool of acid phosphatases could establish as a
57
58 351 result of soil storage. Since the soil was stored for several months before the experiment, it could reach an

1
2
3
4 352 equilibrium at which several enzyme pools with different kinetic characteristics were not needed. It is important to
5
6 353 note that even though the long soil storage very likely affected enzymes concentration as well as other soil
7
8 354 characteristics, it cannot affect our main conclusions because these are based on the kinetic analysis performed
9
10 355 across MUB-P and P-PO₄³⁻ concentrations. Furthermore, all relevant soil characteristics were measured after storage
11
12 356 and before the experiment so the initial reaction conditions were well defined.
13
14

15 357 *Methodological implications*
16

17 358 Both, competitive product inhibition and preferential interaction of acid phosphatases with organic P may
18
19 359 underestimate potential acid phosphatase activity quantified using the standard methodology at certain reaction
20
21 360 conditions (German et al. 2011). Both mechanisms were partly correlated in our study so their individual effects
22
23 361 cannot be determined unambiguously. Also, the estimated values of parameters V_{MAX} , $K_{M-MUB-P}$, K_{ic} , and K_{M-DOP}
24
25 362 should be considered approximate. Because we did not account for any adsorption of P-PO₄³⁻ produced by MUB-P
26
27 363 and organic P decay over time, the inhibitory effect of P-PO₄³⁻ manifested by K_{ic} constant could be underestimated.
28
29 364 We further neglected any transphosphorylation, which would decrease the production rate of P-PO₄³⁻. Also, the
30
31 365 value of K_{M-DOP} could be affected by the activity of phosphodiesterases, which may provide substrate for acid
32
33 366 phosphatases by targeting specific molecules within the organic P pool (Nannipieri et al. 2011). Nevertheless, using
34
35 367 the most accurate model represented by eqs. 6 – 9, we calculated that the underestimation of potential acid
36
37 368 phosphatase activity may range from nearly zero to ~20% of actual potential acid phosphatase activity within the
38
39 369 background inorganic and organic P concentrations 0.1 – 10 $\mu\text{mol g}^{-1}$ (Figure 5; i.e. representing approximate range
40
41 370 of inorganic and organic P concentrations measured across soils – Hou et al. 2018), at initial MUB-P concentration
42
43 371 as high as 300 $\mu\text{mol g(DW)}^{-1}$ and an incubation time one hour. The degree of underestimation could, however, differ
44
45 372 depending on soil P sorption characteristics. It has been shown, that inorganic P sorption is determined by iron (Fe)
46
47 373 and aluminum (Al) oxides in the soils used in this study (Kaňa and Kopáček 2006). In the forest floor and organic
48
49 374 topsoil horizons, the maximum sorption capacity is low due to low content of Fe and Al oxides (Kaňa and Kopáček
50
51 375 2006). As their content increases with depth, the maximum sorption capacity increases and the inhibition of enzyme
52
53 376 reaction by P-PO₄³⁻ is expected to decrease as result. Since the sorption characteristics are further affected by pH
54
55 377 (Kaňa and Kopáček 2006), the opposite is expected along the gradient of increasing soil pH causing increase in
56
57 378 inorganic P availability.
58
59
60
61
62
63
64
65

1
2
3
4
5
6
7
8
9
10
11
12
13
14
15
16
17
18
19
20
21
22
23
24
25
26
27
28
29
30
31
32
33
34
35
36
37
38
39
40
41
42
43
44
45
46
47
48
49
50
51
52
53
54
55
56
57
58
59
60
61
62
63
64
65

379 Several steps in acid phosphatase enzyme assay protocol can be modified to avoid underestimation.
380 However, it is always vital to know the strength of the inhibition as well as inorganic and organic P concentrations.
381 First, background concentration of inorganic and organic P in the final reaction mixture can be minimized by
382 increasing the soil dilution by buffer and by selection of buffer. The citrate buffer used in this study released P from
383 soil (Figure 2) likely due to chelation of Fe and Al oxides (Kaňa and Kopáček 2006) so the initial inorganic P
384 concentration was not zero when no P-PO₄³⁻ was added. A frequently used universal buffer (used in 109 studies
385 published before 2013; Hui et al. 2013) might not be optimal for highly acidic soils either because it is a mixture of
386 citric, maleic and boric acids (Skujins et al. 1962) thus, its P extraction efficiency can be even higher. Lower P
387 extraction efficiency could be theoretically expected from acetate buffer (Wuenschel et al. 2015). The dilution of
388 soil by buffer then needs to be optimized carefully to prevent the excessive dilution of the enzyme (German et al.
389 2011).

390 Based on the inorganic and organic P concentration, and strength of the inhibition, MUB-P concentration
391 and reaction time can be further adjusted to avoid underestimation. When the reaction follows Michaelis-Menten
392 kinetics as generally assumed, the concentration of added MUB-P five times higher than K_M ensures that the
393 measured potential acid phosphatase activity is not less than 83% of V_{MAX} (e.g. Malcolm 1983; Margenot et al.,
394 2018). Since the competitive inhibition increases value of apparent K_M (eq. 2, Figure 1A), the MUB-P concentration
395 must be increased accordingly when inhibition occurs. When only inorganic P inhibits the reaction rate, a short
396 reaction time is recommended to prevent accumulation of the inhibiting product. Short incubation times also
397 minimize the possibility that the microbial and enzyme activities change. On the other hand, when organic P inhibits
398 the reaction rate, too short reaction times should be avoided. In some instances, the concentration of added MUB-P
399 needs to be particularly high to avoid the underestimation. As an example, let's assume that only the competitive
400 inhibition by inorganic P occurs and the K_{ic} value is 50 times lower than K_M (as documented for extracellular acid
401 phosphatase produced by *Cryptococcus neoformans*; Collopy-Junior et al. 2006). To estimate unbiased V_{MAX} within
402 the one hour reaction time (e.g. Blankinship et al. 2014; Marx et al. 2001; Rosinger et al. 2019; Saiya-Cork et al.
403 2002; Schimel et al. 2017; Sistla and Schimel 2013; Weintraub et al. 2007), ~2.5 mmol MUB-P per gram of dry soil
404 has to be added. In terms of amount of organic P, this addition is close to 8% of the entire soil weight. Interestingly,
405 Margenot et al. (2018) recently showed that an even greater concentration of p-nitrophenylphosphate, the alternative
406 to MUB-P, has to be added to some soils to estimate unbiased potential phosphatase activity (~60 mmol per gram of

1
2
3
4 407 dry soil). This recommended concentration is one order magnitude higher than concentrations typically used in the
5
6 408 enzyme assay and could even be inhibitory in some soils (German et al. 2012).

7
8 409 The importance of a saturating concentration of artificial substrate was discussed thoroughly in several
9
10 410 methodological studies (Bell et al. 2013; German et al. 2011; Malcolm 1983; Margenot et al. 2018). According to
11
12 411 our data, however, this concentration could not be always defined well when inhibition is not accounted for. Acid
13
14 412 phosphatase activity estimated within the first five minutes of the reaction time using a linear regression in organic
15
16 413 topsoil horizon from the Čertovo catchment with initial concentrations of inorganic and organic P 10 and 3.5 μmol
17
18 414 $\text{g}(\text{DW})^{-1}$ respectively is shown in Figure 6. Acid phosphatase activity increased with increasing MUB-P
19
20 415 concentration and the resulting hyperbolic relationship could be fitted by eq. 1 with high confidence (adjusted $R^2 =$
21
22 416 0.99). The highest MUB-P concentration could be considered saturating because it was higher than five times the
23
24 417 apparent K_M estimated by eq. 1. The concentration was within the range of concentrations typically used in previous
25
26 418 studies. Also, the acid phosphatase activity at this concentration was undistinguishable from the activity calculated
27
28 419 for the second highest MUB-P concentration (Figure 6). According to all these criteria, V_{MAX} could be estimated with
29
30 420 an error not exceeding 10%. Nevertheless, the kinetic parameters estimated by non-linear analysis of progress curves
31
32 421 suggest that the potential acid phosphatase activity was underestimated by about 20% despite fulfilling seemingly all
33
34 422 recommendations on the reaction parameters. Therefore, non-linear analysis should always be the preferred method
35
36 423 of progress curve analysis because it represents simple and rapid method of inhibition determination (Bezerra and
37
38 424 Dias 2007).

39
40 425 Our results suggest that the V_{MAX} is the same for artificial MUB-P and organic P (Table 3). This result is in
41
42 426 line with expected mechanism of the enzymatic catalysis. If the release of P-PO_4^{3-} group from enzyme active site is
43
44 427 the limiting step of the reaction (Mitić et al. 2006), V_{MAX} should be independent of the substrate identity. Thus, when
45
46 428 carefully conducted, the enzyme activity assay can correctly estimate the maximum activity the pool of acid
47
48 429 phosphatases exhibited in soil under environmental conditions similar to assay conditions. It must be noted,
49
50 430 however, that measured bulk soil conditions might not be always representative to conditions under which the
51
52 431 enzyme operates. The fine scale variability in soil conditions could be large. Depending on whether the enzyme is
53
54 432 located at the surface of clay particles or at the surface of the microbial cell, the pH that the enzyme experiences
55
56 433 could be very different. For example, the difference between the soil solution and exchangeable acidity can be as
57
58 434 high as one pH unit in these soils (Kaňa et al. 2014). It must be also noted that the accurate quantification of V_{MAX} is

1
2
3
4
5
6
7
8
9
10
11
12
13
14
15
16
17
18
19
20
21
22
23
24
25
26
27
28
29
30
31
32
33
34
35
36
37
38
39
40
41
42
43
44
45
46
47
48
49
50
51
52
53
54
55
56
57
58
59
60
61
62
63
64
65

435 not always needed. In many instances, comparison of potential acid phosphatase activity quantified at some standard
436 conditions across different soils or treatments might be sufficient. However, such comparison must be interpreted
437 carefully when differences in background inorganic and/or organic P concentrations are expected.

438 Conclusions

439 Based on all our results discussed above, we recommend to always analyze the progress curve data using a non-
440 linear analysis across the range of initial MUB-P concentrations when the enzyme assay method is optimized for a
441 given soil. When linear regression has to be used, we recommend analyzing residual plots as previously described
442 by Ellis and Duggleby (2015). If the analysis shows the signs of inhibition and the inorganic and/or organic P
443 concentration is expected to change over time, across soil samples or due to experimental treatments, we further
444 recommend to quantify the background concentrations of inorganic and organic P in the medium used to disperse
445 soil. We also suggest to conduct the same analysis with p-nitrophenylphosphate whose decay product is measured
446 colorimetrically. Similar kinetic studies focusing on other enzyme classes should be conducted in other soils to set
447 the limits of possible inhibition constants and thus, help to define reaction conditions at which the unbiased potential
448 enzyme activity could be measured.

449 Funding

450 The research leading to these results received funding from Czech Science Foundation under Grant Agreement No
451 20-14704Y. KT acknowledges support from the Czech Science Foundation project no. 19-16605S.

452 Author contributions

453 All authors contributed to the study conception and design. Data collection and analysis were performed by Petr
454 Čapek. The first draft of the manuscript was written by Petr Čapek and all authors commented on previous versions
455 of the manuscript. All authors read and approved the final manuscript.

1
2
3
4
5
6
7
8
9
10
11
12
13
14
15
16
17
18
19
20
21
22
23
24
25
26
27
28
29
30
31
32
33
34
35
36
37
38
39
40
41
42
43
44
45
46
47
48
49
50
51
52
53
54
55
56
57
58
59
60
61
62
63
64
65

References

Allison SD, Vitousek PM (2005) Responses of extracellular enzymes to simple and complex nutrient inputs. *Soil Biol Biochem* 37:937–944. <https://doi.org/10.1016/j.soilbio.2004.09.014>

Anand A, Srivastava PK (2012) A molecular description of acid phosphatase. *Appl. Biochem. Biotechnol.* 167:2174–2197

Arevalo JR, Carreira JA, Niell FX (1993) Kinetic parameters of phosphatase activity along a xeric dolomitic soil chronosequence related to wildfires. *Geomicrobiol J* 11:235–245. <https://doi.org/10.1080/01490459309377954>

Batistic L, Sarkar JM, Mayaudon J (1980) Extraction, purification and properties of soil hydrolases. *Soil Biol Biochem* 12:59–63. [https://doi.org/10.1016/0038-0717\(80\)90103-0](https://doi.org/10.1016/0038-0717(80)90103-0)

Bell CW, Fricks BE, Rocca JD, Steinweg JM, McMahon SK, Wallenstein MD (2013) High-throughput fluorometric measurement of potential soil extracellular enzyme activities. *J Vis Exp* 50961. <https://doi.org/10.3791/50961>

Bezerra RMF, Dias AA (2007) Utilization of integrated Michaelis-Menten equation to determine kinetic constants. *Biochem Mol Biol Educ* 35:145–150. <https://doi.org/10.1002/bmb.32>

Blankinship JC, Becerra CA, Schaeffer SM, Schimel JP (2014) Separating cellular metabolism from exoenzyme activity in soil organic matter decomposition. *Soil Biol Biochem* 71:68–75. <https://doi.org/10.1016/J.SOILBIO.2014.01.010>

Brookes PC, Landman A, Pruden G, Jenkinson DS (1985) Chloroform fumigation and the release of soil-nitrogen - a rapid direct extraction method to measure microbial biomass nitrogen in soil. *Soil Biol Biochem* 17:837–842. [https://doi.org/10.1016/0038-0717\(85\)90144-0](https://doi.org/10.1016/0038-0717(85)90144-0)

Brookes PC, Powlson DS, Jenkinson DS (1982) Measurement of microbial biomass phosphorus in soil. 1982 14:319–329. [https://doi.org/10.1016/0038-0717\(82\)90001-3](https://doi.org/10.1016/0038-0717(82)90001-3)

Čapek P, Choma M, Tahovská K, Kaňa J, Kopáček J, Šantrůčková H (2021) Coupling the resource stoichiometry and microbial biomass turnover to predict nutrient mineralization and immobilization in soil. *Geoderma* 385:114884. <https://doi.org/10.1016/J.GEODERMA.2020.114884>

Collopy-Junior I, Esteves FF, Nimrichter L, Rodrigues ML, Alviano CS, Meyer-Fernandes JR (2006) An ectophosphatase activity in *Cryptococcus neoformans*. *FEMS Yeast Research* 6: 1010–1017. <https://doi.org/10.1111/j.1567-1364.2006.00105.x>

1
2
3
4 486 Chrost R, Krambeck H (1986) Fluorescence correction for measurements of enzyme activity in natural waters using
5
6 487 methylumbelliferyl-substrates. *Arch für Hydrobiol* 106:79–90
7
8 488 Drouillon M, Merckx R (2005) Performance of para-nitrophenyl phosphate and 4-methylumbelliferyl phosphate as
9
10 489 substrate analogues for phosphomonoesterase in soils with different organic matter content. *Soil Biol Biochem*
11
12 490 37:1527–1534. <https://doi.org/10.1016/j.soilbio.2005.01.008>
13
14 491 Eivazi F, Tabatabai MA (1977) Phosphatases in soils. *Soil Biol Biochem* 9:167–172. <https://doi.org/10.1016/0038->
15
16 492 0717(77)90070-0
17
18 493 Ellis KJ, Duggleby RG (2015) What happens when data are fitted to the wrong equation? *Biochem J* 171:513–517.
19
20 494 <https://doi.org/10.1042/bj1710513d>
21
22 495 German DP, Weintraub MN, Grandy AS, Lauber ChL, Rinkes ZL, Allison SD (2011) Optimization of hydrolytic
23
24 496 and oxidative enzyme methods for ecosystem studies. *Soil Biol Biochem* 43:1387–1397
25
26 497 German DP, Weintraub MN, Grandy AS, Lauber ChL, Rinkes ZL, Allison SD (2012) Response to Steen and
27
28 498 Ziervogel’s comment on “ Optimization of hydrolytic and oxidative enzyme methods to ecosystem studies”
29
30 499 [Soil Biol Biochem 43: 1387-1397]. *Soil Biol Biochem* 48:198–199
31
32 500 Gerritse RG, van Dijk H (1978) Determination of phosphatase activities of soils and animal wastes. *Soil Biol*
33
34 501 *Biochem* 10:545–551. [https://doi.org/10.1016/0038-0717\(78\)90051-2](https://doi.org/10.1016/0038-0717(78)90051-2)
35
36 502 Giesler R, Petersson T, Hogberg P (2002) Phosphorus limitation in boreal forests: Effects of aluminum and iron
37
38 503 accumulation in the humus layer. *Ecosystems* 5:300–314. <https://doi.org/10.1007/s10021-001-0073-5>
39
40 504 Gilboa R, Spungin-Bialik A, Wohlfahrt G, Schomburg D, Blumberg S, Shoham G (2001) Interactions of
41
42 505 *Streptomyces griseus* aminopeptidase with amino acid reaction products and their implications toward a
43
44 506 catalytic mechanism. *Proteins Struct Funct Genet* 44:490–504. <https://doi.org/10.1002/prot.1115>
45
46 507 Gusakov A V., Sinitsyn AP (1992) A theoretical analysis of cellulase product inhibition: Effect of cellulase binding
47
48 508 constant, enzyme/substrate ratio, and β -glucosidase activity on the inhibition pattern. *Biotechnol Bioeng*
49
50 509 40:663–671. <https://doi.org/10.1002/bit.260400604>
51
52 510 Högberg MN, Skjellberg U, Högberg P, Knicker H (2020) Does ectomycorrhiza have a universal key role in the
53
54 511 formation of soil organic matter in boreal forests? *Soil Biol Biochem* 140:107635.
55
56 512 <https://doi.org/10.1016/j.soilbio.2019.107635>
57
58 513 Hou E, Tan X, Heenan M, Wen D (2018) Data descriptor: A global dataset of plant available and unavailable
59
60
61
62
63
64
65

1
2
3
4 514 phosphorus in natural soils derived by hedley method. *Sci Data* 5:1–13. <https://doi.org/10.1038/sdata.2018.166>
5
6 515 Hui D, Mayes MA, Wang G (2013) Kinetic parameters of phosphatase: A quantitative synthesis. *Soil Biol Biochem*
7
8 516 65:105–113. <https://doi.org/10.1016/j.soilbio.2013.05.017>
9
10 517 Juma NG, Tabatabai MA (1988) Comparison of kinetic and thermodynamic parameters of phosphomonoesterases of
11
12 518 soils and of corn and soybean roots. *Soil Biol Biochem* 20:533–539. <https://doi.org/10.1016/0038->
13
14 519 0717(88)90069-7
15
16 520 Kaňa J, Kopáček J (2006) Impact of Soil Sorption Characteristics and Bedrock Composition on Phosphorus
17
18 521 Concentrations in two Bohemian Forest Lakes. *Water Air Soil Pollut* 173:243–259.
19
20 522 <https://doi.org/10.1007/s11270-005-9065-y>
21
22 523 Kaňa J, Šantrůčková H, Kopáček J, Peroutková M, Matějčíková I (2014) Chemical and biochemical characteristics
23
24 524 of soils in the catchments of Čertovo and Plešné lakes (Bohemian Forest) in 2010. *Silva Gabreta* 20:97–129
25
26 525 Kaňa J, Tahovská K, Kopáček J, Šantrůčková H (2015) Excess of organic carbon in mountain spruce forest soils
27
28 526 after bark beetle outbreak altered microbial N transformations and mitigated N-saturation. *PLoS One* 10:1–19.
29
30 527 <https://doi.org/10.1371/journal.pone.0134165>
31
32 528 Kellershohn N, Laurent M (1985) Analysis of progress curves for a highly concentrated Michaelian enzyme in the
33
34 529 presence or absence of product inhibition. *Biochem J* 231:65–74. <https://doi.org/10.1042/bj2310065>
35
36 530 Khadem A, Raiesi F (2019) Response of soil alkaline phosphatase to biochar amendments: Changes in kinetic and
37
38 531 thermodynamic characteristics. *Geoderma* 337:44–54. <https://doi.org/10.1016/j.geoderma.2018.09.001>
39
40 532 Kiffer-Moreira T, Pinheiro AAS, Pinto MR, Esteves FF, Souto-Pradrón T, Barreto-Bergter E, Meyer-Fernandes JR
41
42 533 (2007) Mycelial forms of *Pseudallescheria boydii* present ectophosphatase activities. *Arch Microbiol*
43
44 534 188:159–166. <https://doi.org/10.1007/s00203-007-0232-y>
45
46 535 Kopáček J, Cudlín P, Fluksová H, Kaňa J, Píček T, Šantrůčková H, Svoboda M, Vaněk D (2015) Dynamics and
47
48 536 composition of litterfall in an unmanaged Norway spruce (*Picea abies*) forest after bark-beetle outbreak.
49
50 537 *Boreal Environ Res* 20:305–323
51
52 538 Kopáček J, Hejzlar J (1993) Semi-micro determination of total phosphorus in fresh waters with perchloric acid
53
54 539 digestion. *Int J Environ Anal Chem* 53:173–183. <https://doi.org/10.1080/03067319308045987>
55
56 540 Kopáček J, Turek J, Hejzlar J, Porcal P (2011) Bulk deposition and throughfall fluxes of elements in the Bohemian
57
58 541 Forest (central Europe) from 1998 to 2009. *Boreal Environ Res* 16:495–508
59
60
61
62
63
64
65

- 1
2
3
4 542 Leite MVM, Bobuřská L, Espíndola SP, Campos MRC, Azevedo LCB, Ferreira AS (2018) Modeling of soil
5
6 543 phosphatase activity in land use ecosystems and topsoil layers in the Brazilian Cerrado. *Ecol Modell* 385:182–
7
8 544 188. <https://doi.org/10.1016/j.ecolmodel.2018.07.022>
9
10 545 Malcolm RE (1983) Assessment of phosphatase activity in soils. *Soil Biol Biochem* 15:403–408.
11
12 546 [https://doi.org/10.1016/0038-0717\(83\)90003-2](https://doi.org/10.1016/0038-0717(83)90003-2)
13
14 547 Malik AA, Puissant J, Goodall T, Allison SD, Griffiths RI (2019) Soil microbial communities with greater
15
16 548 investment in resource acquisition have lower growth yield. *Soil Biol Biochem* 132:36–39.
17
18 549 <https://doi.org/10.1016/J.SOILBIO.2019.01.025>
19
20 550 Margenot AJ, Nakayama Y, Parikh SJ (2018) Methodological recommendations for optimizing assays of enzyme
21
22 551 activities in soil samples. *Soil Biol Biochem* 125:350–360. <https://doi.org/10.1016/j.soilbio.2017.11.006>
23
24 552 Marx MC, Wood M, Jarvis SC (2001) A microplate fluorimetric assay for the study of enzyme diversity in soils.
25
26 553 *Soil Biol Biochem* 33:1633–1640. [https://doi.org/10.1016/S0038-0717\(01\)00079-7](https://doi.org/10.1016/S0038-0717(01)00079-7)
27
28 554 Mitić N, Smith SJ, Neves A, Guddat LW, Gahan LR, Schenk G (2006) The catalytic mechanisms of binuclear
29
30 555 metallohydrolases. *Chem. Rev.* 106:3338–3363
31
32 556 Muggeo VMR (2003) Estimating regression models with unknown break-points. *Stat Med* 22:3055–3071
33
34 557 Murphy J, Riley JP (1962) A modified single solution method for determination of phosphate in natural waters. *Anal*
35
36 558 *Chim Acta* 26:31–36
37
38 559 Nannipieri P, Ceccanti B, Cervelli S, Conti C (1982) Hydrolases extracted from soil: Kinetic parameters of several
39
40 560 enzymes catalysing the same reaction. *Soil Biol Biochem* 14:429–432. <https://doi.org/10.1016/0038->
41
42 561 [0717\(82\)90100-6](https://doi.org/10.1016/0038-0717(82)90100-6)
43
44 562 Nannipieri P., Giagnoni L., Landi L., Renella G. (2011) Role of Phosphatase Enzymes in Soil. In: Bünemann E.,
45
46 563 Oberson A., Frossard E. (eds) *Phosphorus in Action. Soil Biology*, vol 26. Springer, Berlin, Heidelberg.
47
48 564 https://doi.org/10.1007/978-3-642-15271-9_9
49
50 565 Nannipieri P, Johnson RL, Paul EA (1978) Criteria for measurement of microbial growth and activity in soil. *Soil*
51
52 566 *Biol Biochem* 10:223–229. [https://doi.org/10.1016/0038-0717\(78\)90100-1](https://doi.org/10.1016/0038-0717(78)90100-1)
53
54 567 Nannipieri P, Trasar-Cepeda C, Dick RP (2018) Soil enzyme activity: a brief history and biochemistry as a basis for
55
56 568 appropriate interpretations and meta-analysis. *Biol Fertil Soils* 54:11–19. <https://doi.org/10.1007/s00374-017->
57
58 569 [1245-6](https://doi.org/10.1007/s00374-017-1245-6)
59
60
61
62
63
64
65

- 1
2
3
4 570 Olander LP, Vitousek PM (2000) Regulation of soil phosphatase and chitinase activity by N and P availability.
5
6 571 Biogeochemistry 49:175–190. <https://doi.org/10.1023/a:1006316117817>
7
8 572 Pang PCK, Kolenko H (1986) Phosphomonoesterase activity in forest soils. *Soil Biol Biochem* 18:35–39.
9
10 573 [https://doi.org/10.1016/0038-0717\(86\)90100-8](https://doi.org/10.1016/0038-0717(86)90100-8)
11
12 574 Perdicakis B, Montgomery HJ, Guillemette JG, Jervis E (2004) Validation and characterization of uninhibited
13
14 575 enzyme kinetics performed in multiwell plates. *Anal Biochem* 332:122–136.
15
16 576 <https://doi.org/10.1016/J.AB.2004.04.023>
17
18 577 R Core Team (2020) R: A Language and Environment for Statistical Computing
19
20 578 Razavi BS, Blagodatskaya E, Kuzyakov Y (2016) Temperature selects for static soil enzyme systems to maintain
21
22 579 high catalytic efficiency. *Soil Biol Biochem* 97:15–22. <https://doi.org/10.1016/j.soilbio.2016.02.018>
23
24 580 Reytor González ML, Cornell-Kennon S, Schaefer E, Kuzmič P (2017) An algebraic model to determine substrate
25
26 581 kinetic parameters by global nonlinear fit of progress curves. *Anal Biochem* 518:16–24.
27
28 582 <https://doi.org/10.1016/J.AB.2016.11.001>
29
30 583 Rosinger C, Rousk J, Sandén H (2019) Can enzymatic stoichiometry be used to determine growth-limiting nutrients
31
32 584 for microorganisms? - A critical assessment in two subtropical soils. *Soil Biol Biochem* 128:115–126.
33
34 585 <https://doi.org/10.1016/J.SOILBIO.2018.10.011>
35
36 586 Saiya-Cork KR, Sinsabaugh RL, Zak DR (2002) The effects of long term nitrogen deposition on extracellular
37
38 587 enzyme activity in an *Acer saccharum* forest soil. *Soil Biol Biochem* 34:1309–1315.
39
40 588 [https://doi.org/10.1016/S0038-0717\(02\)00074-3](https://doi.org/10.1016/S0038-0717(02)00074-3)
41
42 589 Šantrůčková H, Vrba J, Pícek T, Kopáček J (2004) Soil biochemical activity and phosphorus transformations and
43
44 590 losses from acidified forest soils. *Soil Biol Biochem* 36:1569–1576.
45
46 591 <https://doi.org/10.1016/j.soilbio.2004.07.015>
47
48 592 Schimel J, Becerra CA, Blankinship J (2017) Estimating decay dynamics for enzyme activities in soils from
49
50 593 different ecosystems. *Soil Biol Biochem* 114:5–11. <https://doi.org/10.1016/j.soilbio.2017.06.023>
51
52 594 Sinsabaugh RL, Manzoni S, Moorhead DL, Richter A, Elser J (2013) Carbon use efficiency of microbial
53
54 595 communities: stoichiometry, methodology and modelling. *Ecol Lett* 16:930–939.
55
56 596 <https://doi.org/10.1111/ele.12113>
57
58 597 Sistla SA, Schimel JP (2013) Seasonal patterns of microbial extracellular enzyme activities in an arctic tundra soil:
59
60
61
62
63
64
65

1
2
3
4 598 Identifying direct and indirect effects of long-term summer warming. *Soil Biol Biochem* 66:119–129.
5
6 599 <https://doi.org/10.1016/j.soilbio.2013.07.003>
7
8 600 Skujins JJ, Braal L, McLaren AD (1962) Characterization of phosphatase in a terrestrial soil sterilized with an
9
10 601 electron beam. *Enzymologia* 25:125–133
11
12 602 Soetaert K, Petzoldt T, Setzer RW (2010) Solving Differential Equations in R: Package deSolve. *J Stat Softw* 33:1–
13
14 603 25. <https://doi.org/10.18637/jss.v033.i09>
15
16 604 Spiers GA, McGill WB (1979) Effects of phosphorus addition and energy supply on acid phosphatase production
17
18 605 and activity in soils. *Soil Biol Biochem* 11:3–8. [https://doi.org/10.1016/0038-0717\(79\)90110-X](https://doi.org/10.1016/0038-0717(79)90110-X)
19
20 606 Steen AD, Ziervogel K (2012) Comment on the review by German et al. (2011) “ Optimization of hydrolytic and
21
22 607 oxidative enzyme methods for ecosystem studies” [*Soil Biol Biochem* 43: 1387-1397]. *Soil Biol Biochem*
23
24 608 48:196–197
25
26 609 Stock SC, Köster M, Dippold MA, Nájera F, Matus F, Merino C, Boy J, Spielvogel S, Gorbushina A, Kuzyakov Y
27
28 610 (2019) Environmental drivers and stoichiometric constraints on enzyme activities in soils from rhizosphere to
29
30 611 continental scale. *Geoderma* 337:973–982. <https://doi.org/10.1016/j.geoderma.2018.10.030>
31
32 612 Stone MM, Plante AF (2014) Changes in phosphatase kinetics with soil depth across a variable tropical landscape.
33
34 613 *Soil Biol Biochem* 71:61–67. <https://doi.org/10.1016/j.soilbio.2014.01.006>
35
36 614 Sunden F, Alsadhan I, Lyubimov AY, Ressler S, Wiersma-Koch H, Borland J, Brown CL, Johnson TA, Singh Z,
37
38 615 Herschlag D (2016) Mechanistic and Evolutionary Insights from Comparative Enzymology of
39
40 616 Phosphomonoesterases and Phosphodiesterases across the Alkaline Phosphatase Superfamily. *J Am Chem Soc*
41
42 617 138:14273–14287. <https://doi.org/10.1021/jacs.6b06186>
43
44 618 Tahovská K, Čapek P, Šantrůčková H, Kopáček J (2018) In situ phosphorus dynamics in soil: long-term ion-
45
46 619 exchange resin study. *Biogeochemistry* 1–14. <https://doi.org/10.1007/s10533-018-0470-x>
47
48 620 Tahovská K, Kaňa J, Bárta J, Oulehle F, Richter A, Šantrůčková H (2013) Microbial N immobilization is of great
49
50 621 importance in acidified mountain spruce forest soils. *Soil Biol Biochem* 59:58–71.
51
52 622 <https://doi.org/10.1016/j.soilbio.2012.12.015>
53
54 623 Tan X, Machmuller MB, Huang F, He J, Chen J, Cotrufo MF, Shen W (2020) Temperature sensitivity of ecoenzyme
55
56 624 kinetics driving litter decomposition: The effects of nitrogen enrichment, litter chemistry, and decomposer
57
58 625 community. *Soil Biol Biochem* 148:107878. <https://doi.org/10.1016/j.soilbio.2020.107878>
59
60
61
62
63
64
65

1
2
3
4 626 Trasar-Cepeda C, Gil-Sotres F, Leiros MC (2007) Thermodynamic parameters of enzymes in grassland soils from
5
6 627 Galicia, NW Spain. *Soil Biol Biochem* 39:311–319. <https://doi.org/10.1016/j.soilbio.2006.08.002>
7
8 628 Trasar-Cepeda MC, Gil-Sotres F (1988) Kinetics of acid phosphatase activity in various soils of Galicia (NW Spain).
9
10 629 *Soil Biol Biochem* 20:275–280. [https://doi.org/10.1016/0038-0717\(88\)90003-X](https://doi.org/10.1016/0038-0717(88)90003-X)
11
12 630 Turek J, Fluksová H, Hejzlar J, Kopáček J, Porcal P (2014) Modelling air temperature in catchments of Čertovo and
13
14 631 Plešné lakes in the Bohemian Forest back to 1781. *Silva Gabreta* 20:1–24
15
16 632 Vance ED, Brookes PC, Jenkinson DS (1987) An extraction method for measuring soil microbial biomass-C. *Soil*
17
18 633 *Biol Biochem* 19:703–707. [https://doi.org/10.1016/0038-0717\(87\)90052-6](https://doi.org/10.1016/0038-0717(87)90052-6)
19
20 634 Vega Yon G, Muñoz E (2017) ABCoptim: An implementation of the Artificial Bee Colony (ABC) Algorithm
21
22 635 Verchot L V., Borelli T (2005) Application of para-nitrophenol (pNP) enzyme assays in degraded tropical soils. *Soil*
23
24 636 *Biol Biochem* 37:625–633. <https://doi.org/10.1016/j.soilbio.2004.09.005>
25
26 637 Vötsch W, Templin MF (2000) Characterization of a beta-N-acetylglucosaminidase of *Escherichia coli* and
27
28 638 elucidation of its role in muropeptide recycling and beta-lactamase induction. *J Biol Chem* 275:39032–8.
29
30 639 <https://doi.org/10.1074/jbc.M004797200>
31
32 640 Vuorinen AH (1999) Phosphatases in horse and chicken manure composts. *Compost Sci Util* 7:47–54.
33
34 641 <https://doi.org/10.1080/1065657X.1999.10701963>
35
36 642 Vuorinen AH, Saharinen MH (1996) Effects of soil organic matter extracted from soil on acid
37
38 643 phosphomonoesterase. *Soil Biol Biochem* 28:1477–1481. [https://doi.org/10.1016/S0038-0717\(96\)00166-6](https://doi.org/10.1016/S0038-0717(96)00166-6)
39
40 644 Weintraub MN, Scott-Denton LE, Schmidt SK, Monson RK (2007) The effects of tree rhizodeposition on soil
41
42 645 exoenzyme activity, dissolved organic carbon, and nutrient availability in a subalpine forest ecosystem.
43
44 646 *Oecologia* 154:327–338. <https://doi.org/10.1007/s00442-007-0804-1>
45
46 647 Wuenscher R, Unterfrauner H, Peticzka R, Zehetner F (2015) A comparison of 14 soil phosphorus extraction
47
48 648 methods applied to 50 agricultural soils from Central Europe. *Plant, Soil Environ* 61:86–96.
49
50 649 <https://doi.org/10.17221/932/2014-PSE>
51
52 650 Yoshida K, Ogawa N, Oshima Y (1989) Function of the PHO regulatory genes for repressible acid phosphatase
53
54 651 synthesis in *Saccharomyces cerevisiae*. *MGG Mol Gen Genet* 217:40–46.
55
56 652 <https://doi.org/10.1007/BF00330940>
57
58 653 Zhang X, Yang Y, Zhang C, Niu S, Yang H, Yu G, Wang H, Blagodatskaya E, Kuzyakov Y, Tian D, Tang Y, Liu S,
59
60
61
62
63
64
65

1
2
3
4
5
6
7
8
9
10
11
12
13
14
15
16
17
18
19
20
21
22
23
24
25
26
27
28
29
30
31
32
33
34
35
36
37
38
39
40
41
42
43
44
45
46
47
48
49
50
51
52
53
54
55
56
57
58
59
60
61
62
63
64
65

654 Sun X (2018) Contrasting responses of phosphatase kinetic parameters to nitrogen and phosphorus additions
655 in forest soils. *Funct Ecol* 32:106–116. <https://doi.org/10.1111/1365-2435.12936>

656

14
15
16
17
18
19
20
21
22
23
24
25
26
27
28
29
30
31
32
33
34
35
36
37
38
39
40
41
42
43
44
45
46
47
48
49
50
51
52
53
54
55
56
57
58
59
60
61
62
63
64
65

657 **Tables**

658 **Table 1:** Basic chemical (C_T – total soil organic C content, N_T – total soil N content, DOC – K_2SO_4 extractable organic C, DON – K_2SO_4 extractable organic N,
659 NH_4^+ – K_2SO_4 extractable ammonium, NO_3^- – K_2SO_4 extractable nitrate, SRP – citrate-buffer extractable soluble reactive P, DOP – citrate-buffer extractable
660 organic P) and microbiological (MBC – microbial biomass C, MBN – microbial biomass N, MBP – microbial biomass P) characteristics of forest floor and
661 organic topsoil horizons sampled in October 2019 in mountain spruce forest catchments of glacier lakes Plešné and Čertovo.

Catchment	Horizon	pH	C_T %	N_T	DOC	DON	NH_4^+	NO_3^-	SRP $\mu\text{mol g}^{-1}$	DOP	MBC	MBN	MBP
Plešné	Forest floor	4.51	47.0	1.86	71.1	24.2	83.9	3.69	2.83	3.97	863	42,2	12.1
					<i>3.48</i>	<i>0.74</i>	<i>0.56</i>	<i>0,11</i>	<i>1.43</i>	<i>1.61</i>	<i>55.5</i>	<i>13.7</i>	<i>0.85</i>
Plešné	Organic topsoil	3.58	42.9	1.57	64.9	49.6	33.2	3.15	2.04	2,42	766	28.3	9.87
					<i>1.86</i>	<i>4.62</i>	<i>3.23</i>	<i>0.25</i>	<i>0.79</i>	<i>1.37</i>	<i>26.6</i>	<i>11.5</i>	<i>1.09</i>
Čertovo	Forest floor	4.06	38.1	2.03	90.4	128	93.4	7.49	2.19	3.15	851	40.8	14.4
					<i>5.79</i>	<i>1.87</i>	<i>0.29</i>	<i>0.05</i>	<i>0.99</i>	<i>1.92</i>	<i>16.3</i>	<i>4.71</i>	<i>4.39</i>
Čertovo	Organic topsoil	3.61	49.3	1.53	41.7	39.3	23.6	5.37	1.41	2.23	627	28.7	5.81
					<i>0.97</i>	<i>1.53</i>	<i>0.59</i>	<i>0.18</i>	<i>0.78</i>	<i>1.08</i>	<i>42.6</i>	<i>1.79</i>	<i>0.52</i>

662

1
2
3
4 **663** **Table 2:** Results of non-linear least square regression conducted with four different equations representing
5
6 **664** Michaelis-Menten kinetics without the inhibition (WI), with competitive product inhibition (CI), noncompetitive
7
8 **665** product inhibition (NCI) and uncompetitive product inhibition (UCI). Equations were fitted to the MUB-P decay
9
10 **666** progress curve data acquired for two different soil horizons (forest floor and topsoil organic horizon) sampled in two
11
12 **667** catchments (Plešné and Čertovo). SS_{RES} – residual sum of squares, LLR – log likelihood ratio comparing the fit of a
13
14 **668** respective model with WI model. Symbols above the numbers denote the probability that a respective model fits the
15
16 **669** data better than WI model ($***p < 0.001$, $**p < 0.01$, $*p < 0.05$).

Catchment	Horizon	Model	SS _{RES}	LLR
Plešné	Forest floor	WI	9914	
		CI	6037	818***
		NCI	7800	396***
		UCI	9772	24***
Plešné	Organic topsoil	WI	43434	
		CI	17218	1107***
		NCI	30852	566***
		UCI	30852	566***
Čertovo	Forest floor	WI	51360	
		CI	24677	978***
		NCI	42427	300***
		UCI	51189	20***
Čertovo	Organic topsoil	WI	51020	
		CI	14783	2230***
		NCI	46004	167***
		UCI	42760	420***

41 **670**

44 **671**

Table 3: Parameters and goodness of fit of three models simulating the increase of reaction product of MUB-P decay over time. The models acknowledge competitive product inhibition (CI), inhibition by preferential interaction of organic P with acid phosphatases (eqs. 3 - 5) and combination of both types of inhibition (eqs. 6 – 9). Models were parametrized against the product concentration of the MUB-P decay acquired for two different soil horizons (forest floor and topsoil organic horizon) sampled in two catchments (Plešné and Čertovo). V_{MAX} – maximum velocity constant ($\mu\text{mol g}^{-1} \text{min}^{-1}$), $K_{M-MUB-P}$ – apparent affinity constant for MUB-P ($\mu\text{mol g}^{-1}$), K_{M-DOP} – apparent affinity constant for organic P[†] ($\mu\text{mol g}^{-1}$), K_{ic} – apparent inhibition constant ($\mu\text{mol g}^{-1}$), SS_{res} – residual sum of squares, LLR – log likelihood ratio comparing the goodness of fit of a respective model with CI model. The best model is highlighted by bold face. Symbols above the numbers denote the probability that a respective model fits the data better than CI model (*** $p < 0.001$, ** $p < 0.01$, * $p < 0.05$).

Catchment	Horizon	Model	Parameters				SS _{RES}	LLR
			V_{MAX}	$K_{M-MUB-P}$	K_{M-DOP}	K_{ic}		
Plešné	Forest floor	CI	0.17	15.9		21.8	0.185	
		Eqs. 3 - 5	0.14	13.0	3.3		0.118	6.39**
		Eqs. 6 - 9	0.13	10.9	4.0	164.9	0.139	4.31*
Plešné	Organic topsoil	CI	0.06	11.4		18.3	0.040	
		Eqs. 3 - 5	0.05	8.7	3.8		0.048	-2,97
		Eqs. 6 - 9	0.05	8.8	208.7	16.5	0.033	3.18*
Čertovo	Forest floor	CI	0.26	22.6		19.7	0.298	
		Eqs. 3 - 5	0.13	9.9	3.8		0.556	-20,9
		Eqs. 6 - 9	0.18	14.2	3.9	105.0	0.233	5.28*
Čertovo	Organic topsoil	CI	0.06	4.7		10.7	0.064	
		Eqs. 3 - 5	0.05	3.3	1.3		0.061	0,50
		Eqs. 6 - 9	0.06	4.0	1.7	55.3	0.042	3.83*

[†]Citrate buffer extractable organic P

1
2
3
4
5
6
7
8
9
10
11
12
13
14
15
16
17
18
19
20
21
22
23
24
25
26
27
28
29
30
31
32
33
34
35
36
37
38
39
40
41
42
43
44
45
46
47
48
49
50
51
52
53
54
55
56
57
58
59
60
61
62
63
64
65

684 Figure captions

685 Fig. 1 A) Relationship between artificial substrate concentration and uninhibited (grey line) or inhibited enzyme
686 activity (black line). The equations describing uninhibited and competitively inhibited enzyme reaction are reported
687 in the figure and denoted by different colors. In both equations, $V_{MAX} = 5 \mu\text{mol g}^{-1} \text{h}^{-1}$ (represented by thin horizontal
688 line) and $K_M = 25 \mu\text{mol g}^{-1}$. The concentration of inhibitor and value of inhibition constant (K_{ic}) is reported in the
689 figure. B) Increase of fluorescent (i.e. MUB – circles) and inhibiting (squares) product over four hours incubation
690 time following the uninhibited (grey color) or inhibited enzyme activity kinetic (black color) visualized in panel A.
691 Solid lines of different colors represent visualization of the linear regression conducted with the data, whose slope
692 should approach V_{MAX} . C) Slope of linear regression visualized in panel B

693 Fig. 2 A) Inorganic P in soil-buffer slurry at five concentrations of added P-PO_4^{3-} . Circles represent forest floor
694 horizons, whereas squares represent organic topsoil horizons. Black and grey colors of the symbols represent soils
695 from Plešné and Čertovo catchments, respectively. Solid line represent 1:1 relationship and the dashed line a linear
696 relationship drawn across all data. B) Dissolved organic P in soil-buffer slurry at three concentrations of added P-
697 PO_4^{3-} . Black bars represent forest floor horizons, whereas grey bars represent organic topsoil horizons. A height of
698 the bar represent the mean organic P concentration and error bars are standard deviations of the mean

699 Fig 3 Relative acid phosphatase activity. It was calculated for each initial concentration of MUB-P and inorganic P
700 as a percentage in respect to acid phosphatase activity when no P-PO_4^{3-} was added to respective MUB-P. Symbols
701 represent means and error bars represent standard errors of the mean. Solid/dashed lines represent the estimation by
702 the competitive product inhibition model. Different symbols' and lines' colors denote different initial concentrations
703 of MUB-P. Figure is divided into four boxes representing four soils used in this study

704 Fig. 4 Acid phosphatase activity calculated for two time intervals. The two time intervals are denoted by different
705 colors of the bars and were defined by a piecewise linear regression. Numbers in the bars denote the breakpoint
706 dividing the entire reaction time into two intervals. The bars represent mean values and error bars represent standard
707 error of the mean. Figure is divided into two boxes representing two soil horizons from Plešné and Čertovo
708 catchments. Note that boxes have different y-axis scales

709 Fig. 5 The effect of initial inorganic P and organic P concentrations on acid phosphatase activity estimated by a
710 standard assay in forest floor (solid lines) and organic topsoil (dashed lines) horizons from Plešné and Čertovo

1
2
3
4
5
6
7
8
9
10
11
12
13
14
15
16
17
18
19
20
21
22
23
24
25
26
27
28
29
30
31
32
33
34
35
36
37
38
39
40
41
42
43
44
45
46
47
48
49
50
51
52
53
54
55
56
57
58
59
60
61
62
63
64
65

711 catchments. A) The effect of inorganic P at two concentrations of organic P denoted by black and grey line colors.

712 B) The effect of organic P at two concentrations of inorganic P denoted by black and grey line colors. In all

713 simulations, added amount of MUB-P is $300 \mu\text{mol g(DW)}^{-1}$ and the reaction time is one hour

714 **Fig. 6** Relationship between the initial MUB-P concentration and acid phosphatase activity. The symbols represent

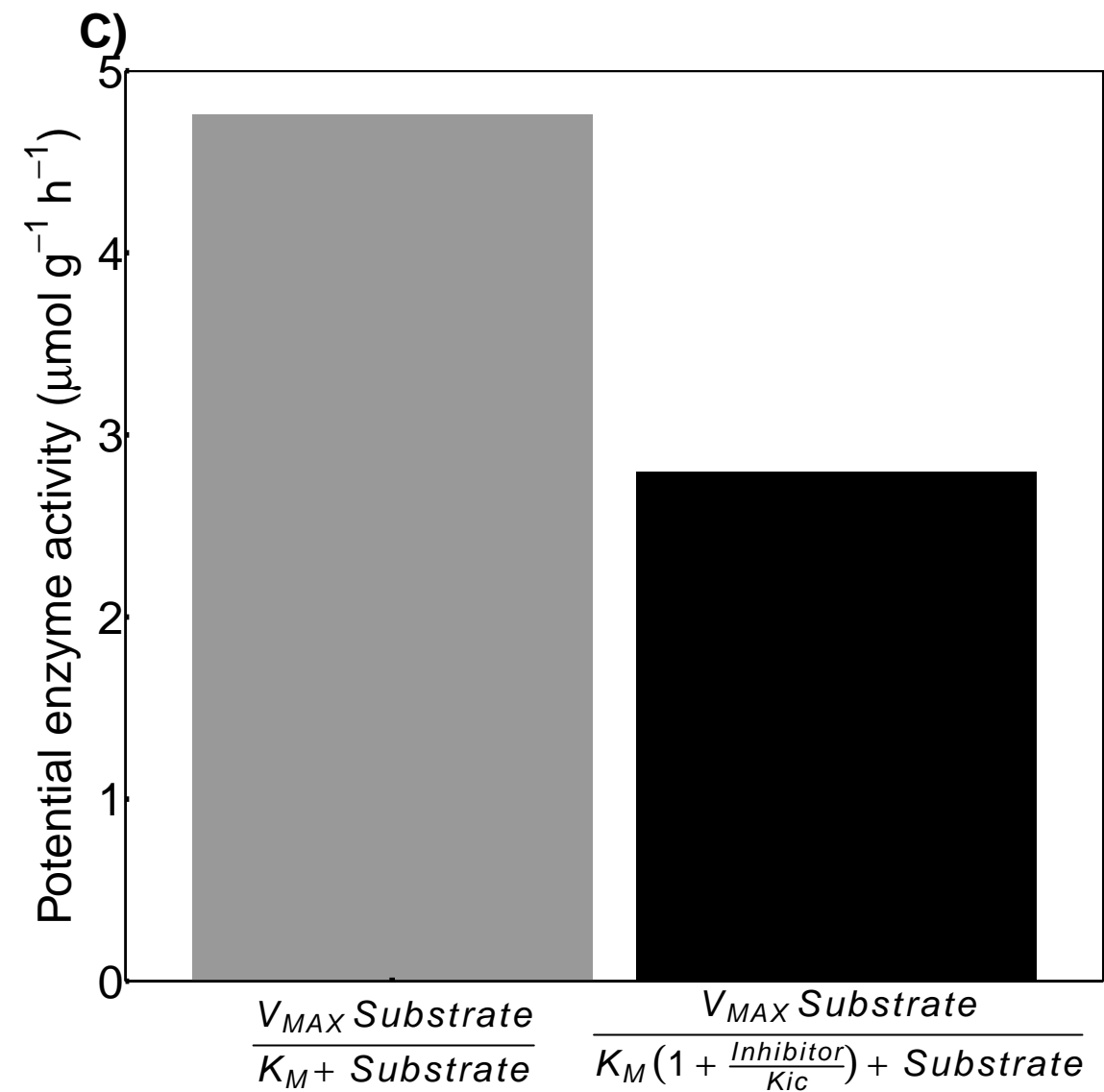
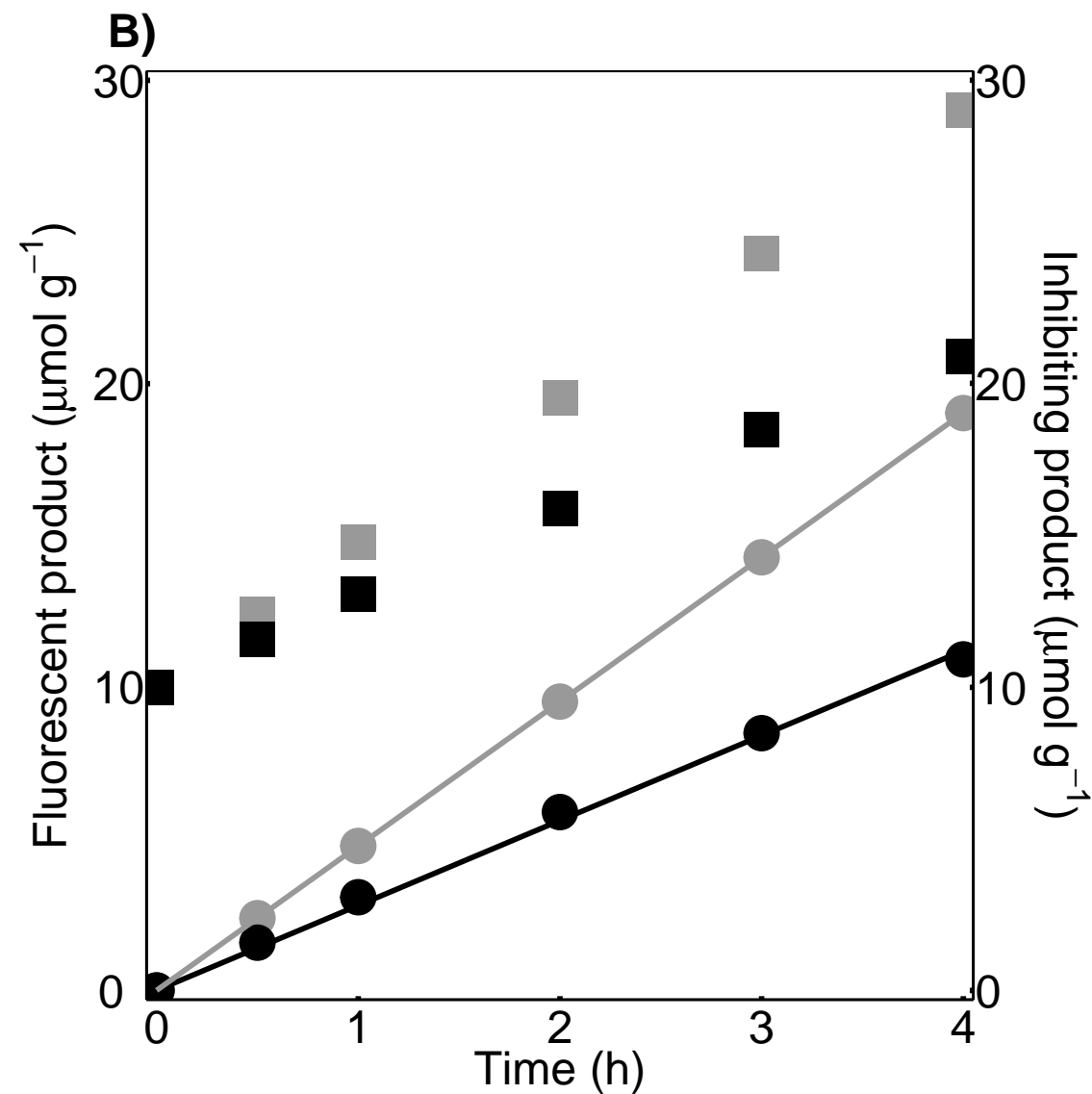
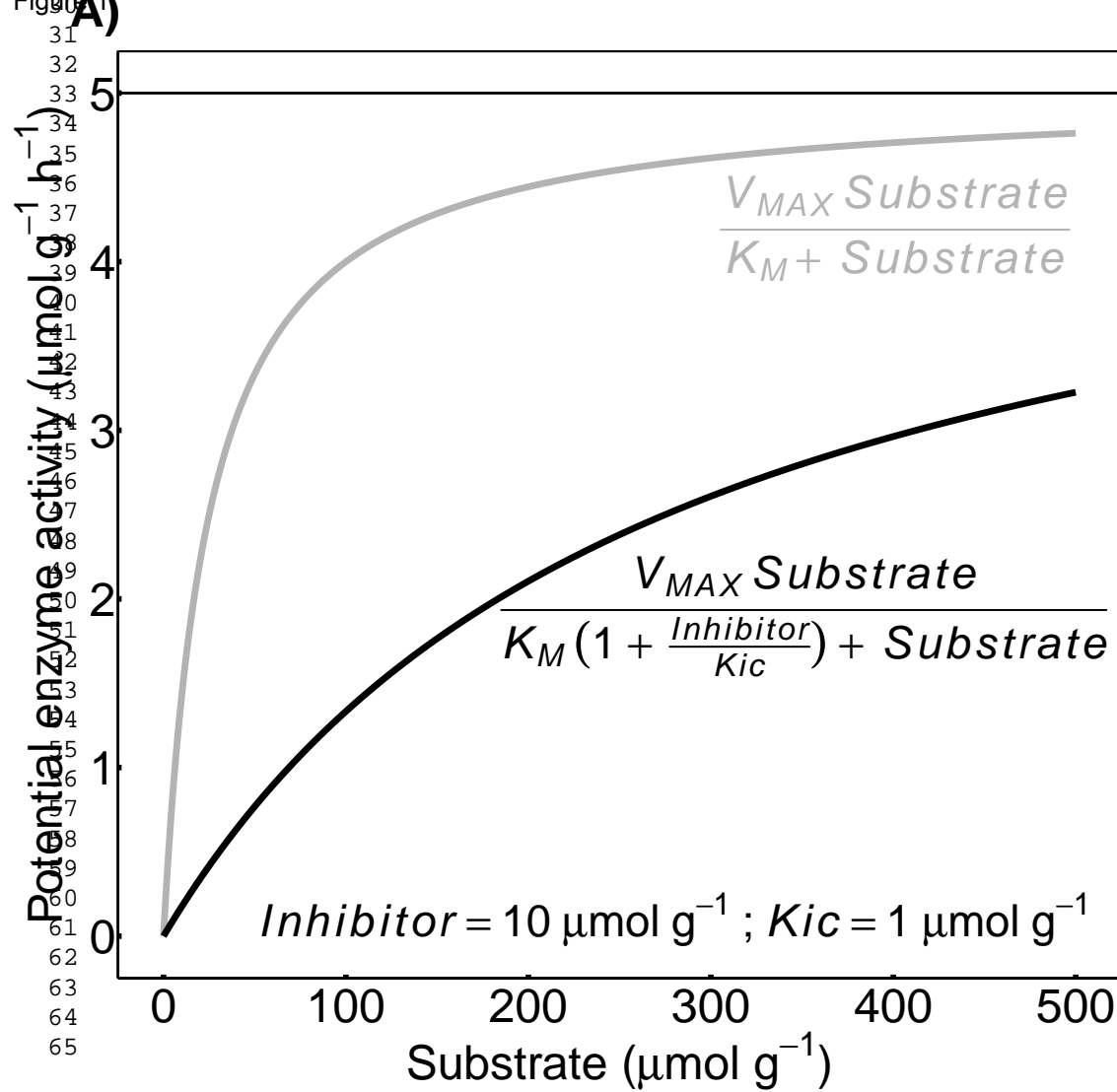
715 estimates calculated for organic topsoil from Čertovo catchment at initial inorganic and organic P concentrations 10

716 and $3.5 \mu\text{mol g}^{-1}$, respectively. The estimates were calculated using a linear regression conducted within the first five

717 minutes of the reaction time. Black solid line represents the fit of Michaelis-Menten equation without the inhibition.

718 Grey line represents the Michaelis-Menten kinetics at zero inorganic and organic P concentration based on the

719 equation parameters reported in Table 3. Error bars represent standard error of linear regression estimate



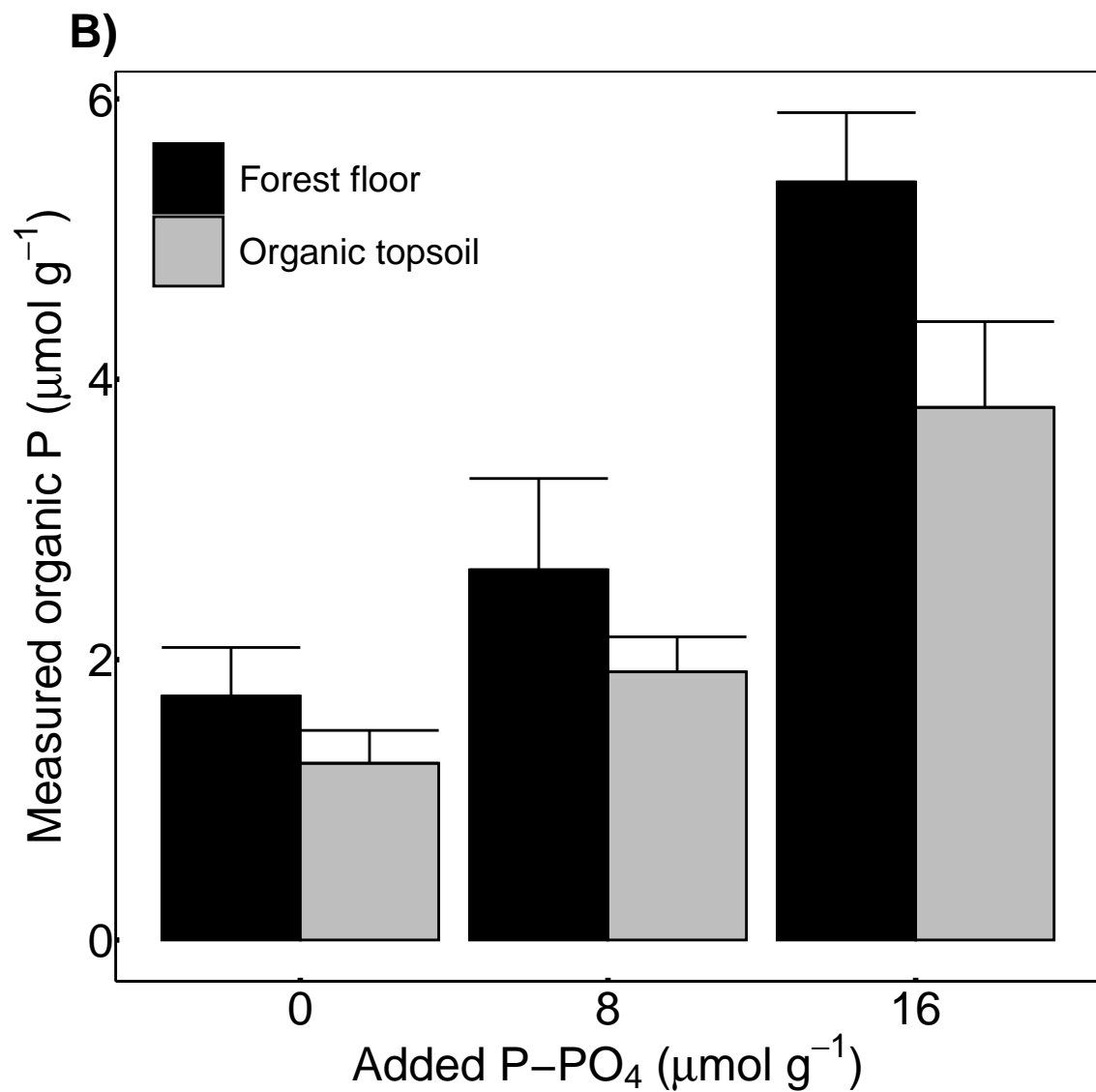
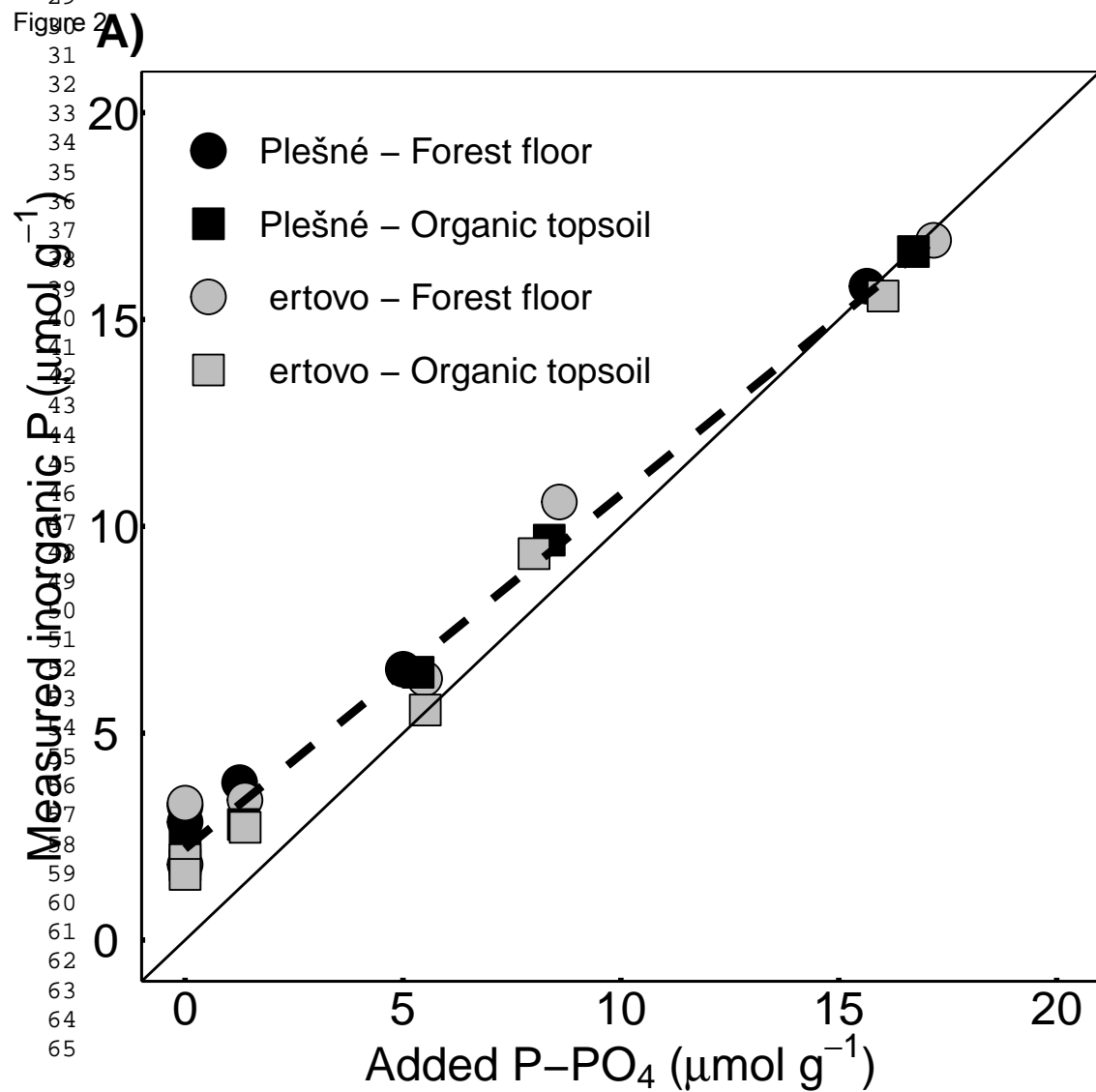


Figure 3
31
32
33
34
35
36
37
38
39
40
41
42
43
44
45
46
47
48
49
50
51
52
53
54
55
56
57
58
59
60
61
62
63
64
65

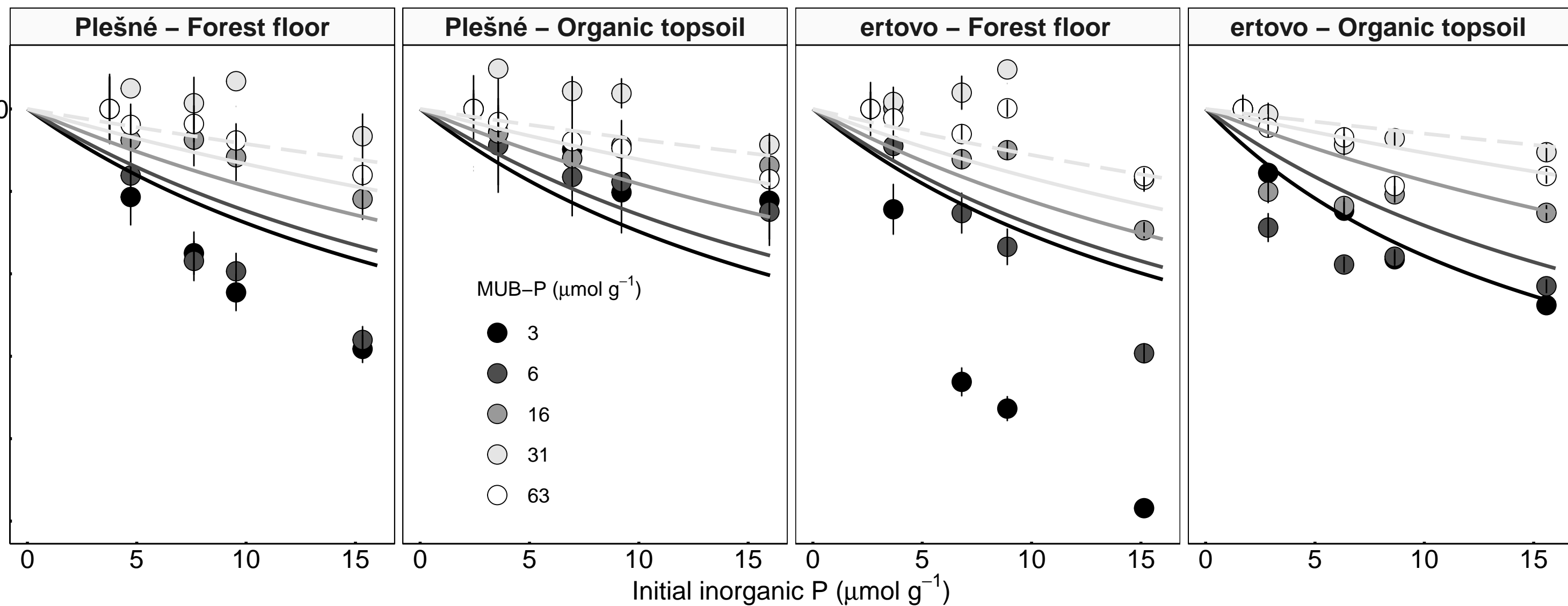


Figure 4
31
32
33
34
35
36
37
38
39
40
41
42
43
44
45
46
47
48
49
50
51
52
53
54
55
56
57
58
59
60
61
62
63
64
65

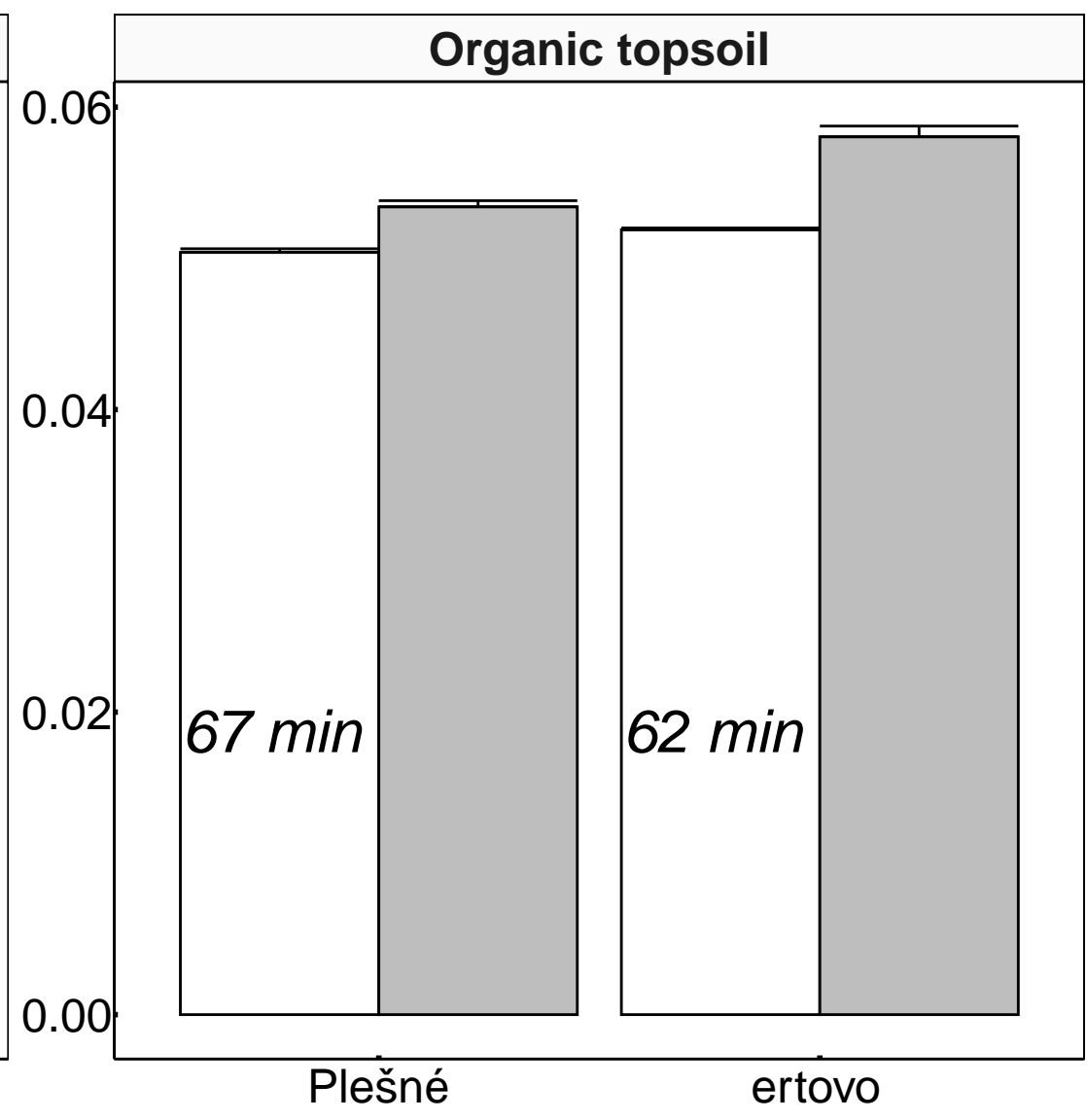
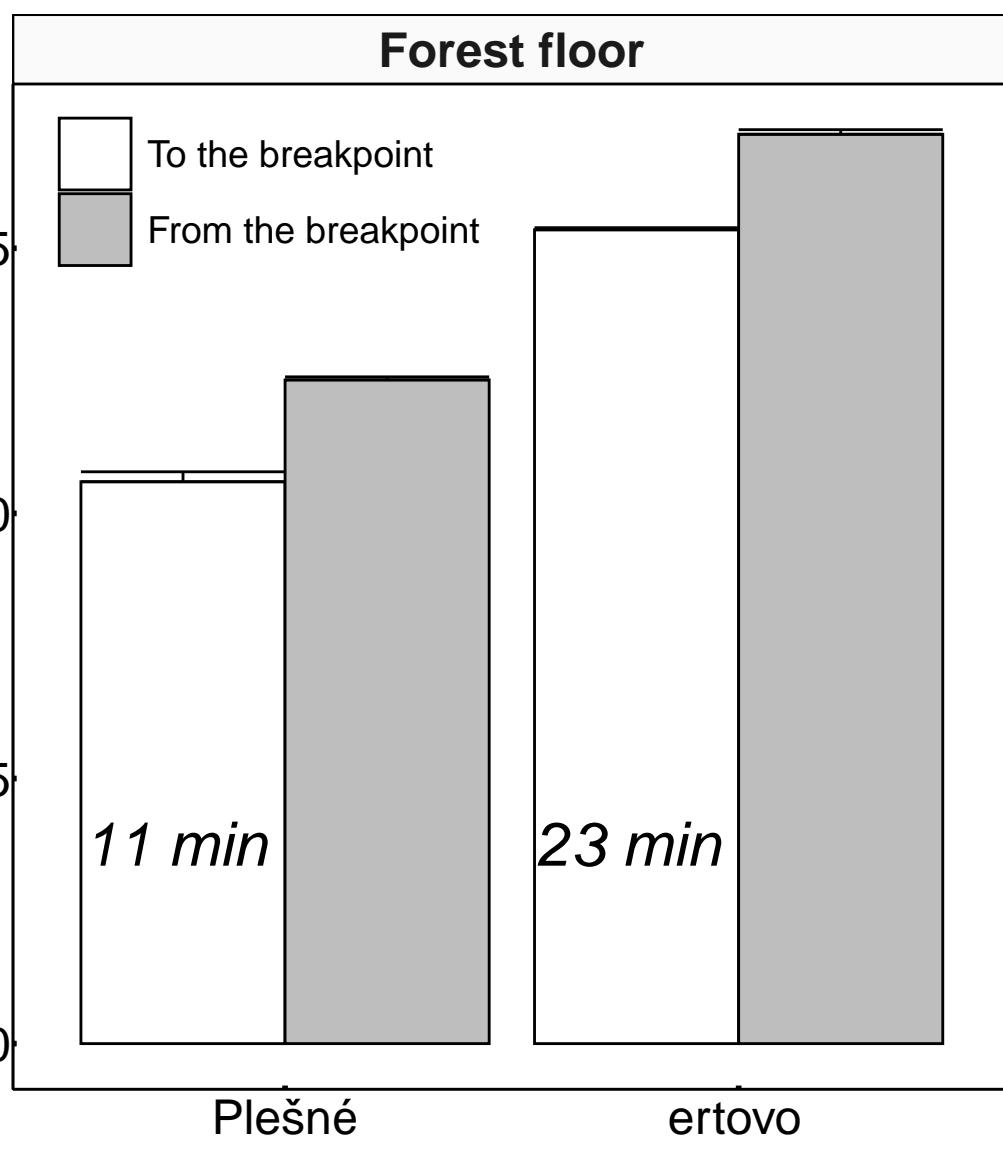


Figure 5

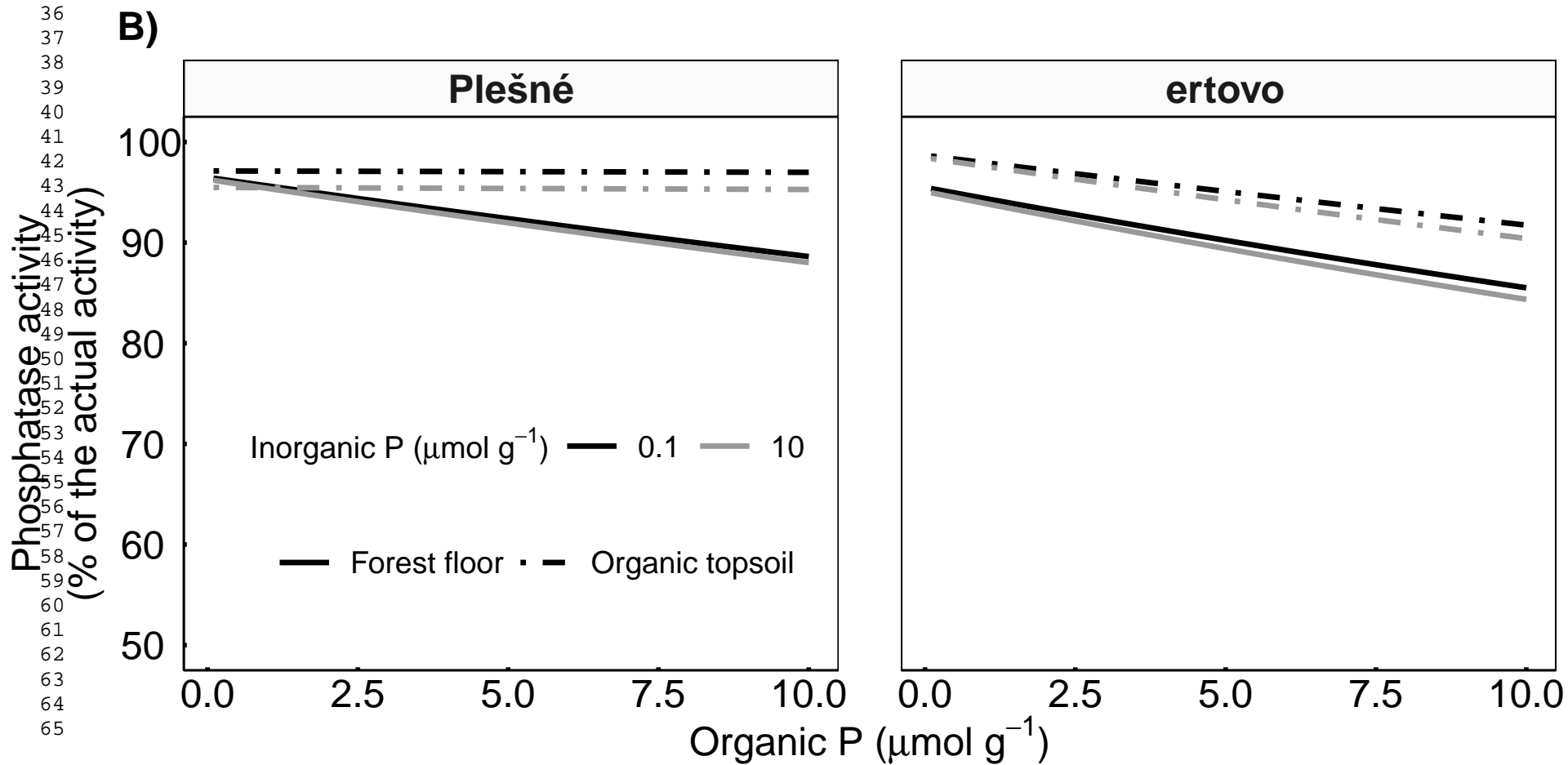
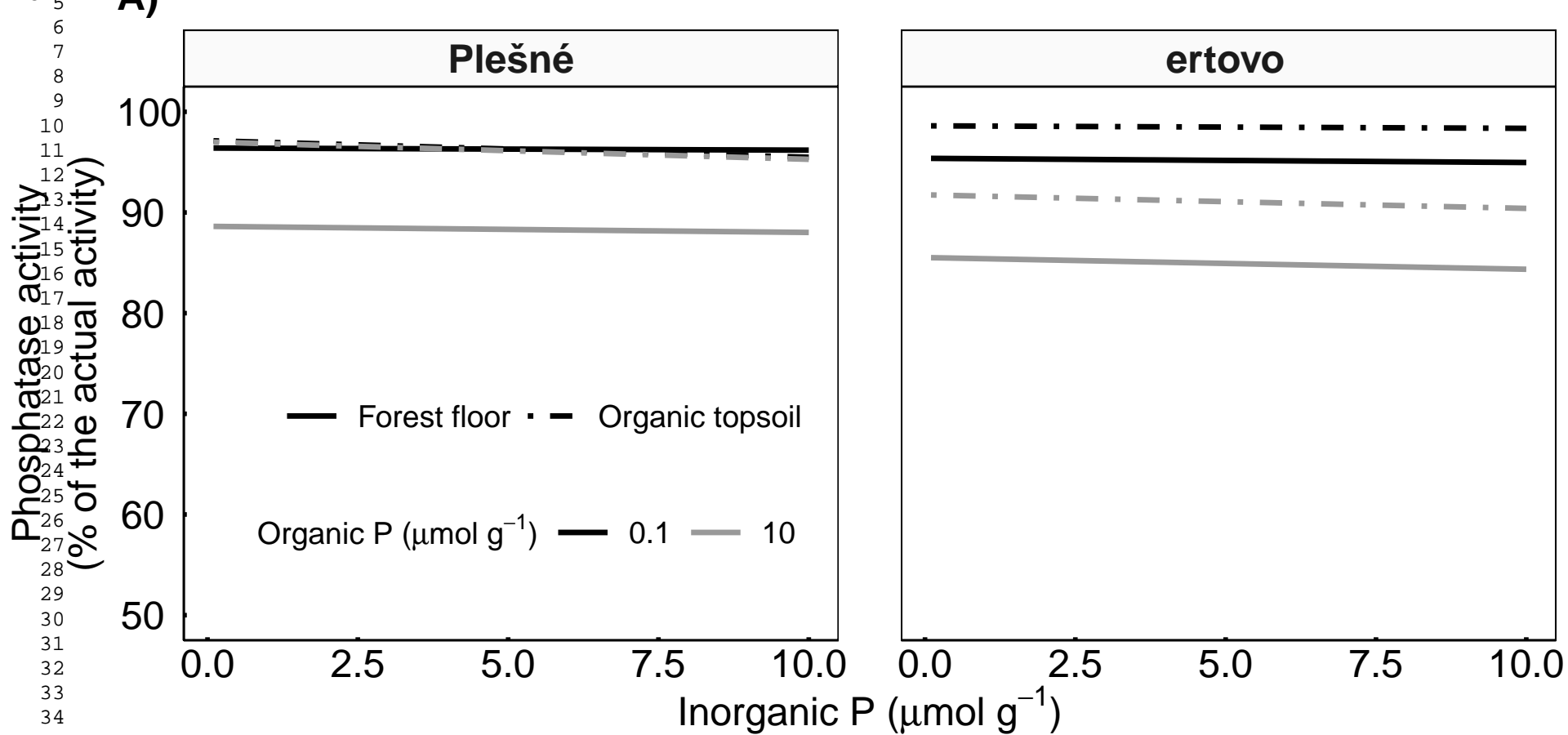
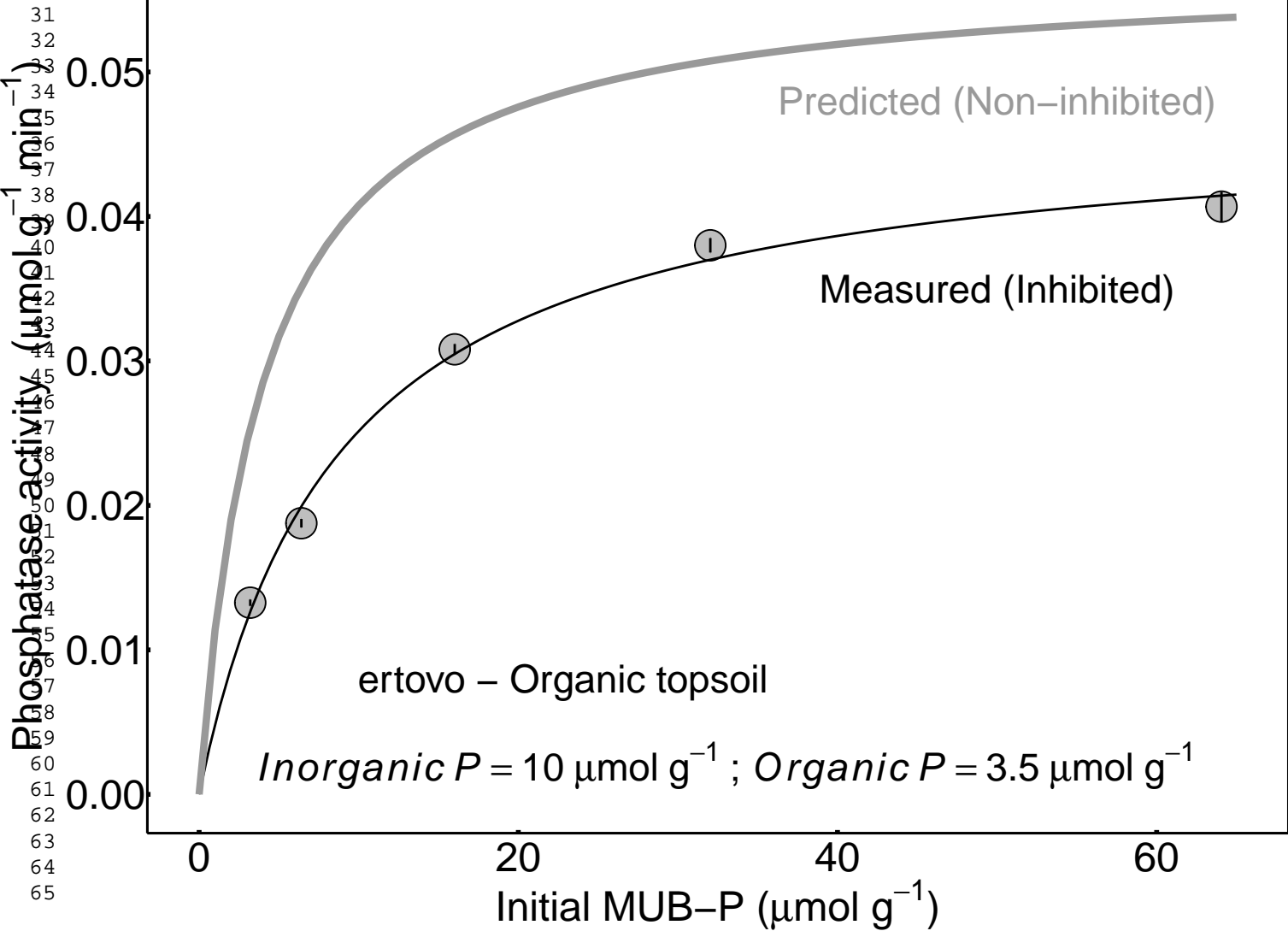
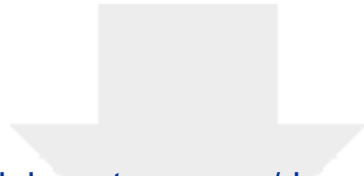


Figure 6



31
32
33
34
35
36
37
38
39
40
41
42
43
44
45
46
47
48
49
50
51
52
53
54
55
56
57
58
59
60
61
62
63
64
65



Click here to access/download

Electronic Supplementary Material
e_supp_material_BFS_revised.pdf

